MOLECULAR METABOLISM

CrossMark

Adipocyte progenitor cells initiate monocyte chemoattractant protein-1-mediated macrophage accumulation in visceral adipose tissue

Jennifer L. Kaplan [1,2], Melissa A. Marshall [1], Chantel C. McSkimming [1], Daniel B. Harmon [1,3], James C. Garmey [1], Stephanie N. Oldham [1], Peter Hallowell [4], Coleen A. McNamara [1,5,6,7,*]

ABSTRACT

Objective: Macrophages are important producers of obesity-induced MCP-1; however, initial obesity-induced increases in MCP-1 production precede M1 macrophage accumulation in visceral adipose tissue (VAT). The initial cellular source of obesity-induced MCP-1 *in vivo* is currently unknown. Preliminary reports based on *in vitro* studies of preadipocyte cell lines and adherent stroma-vascular fraction cells suggest that resident stromal cells express MCP-1. In the past several years, elegant methods of identifying adipocyte progenitor cells (AdPCs) have become available, making it possible to study these cells *in vivo*. We have previously published that global deletion of transcription factor Inhibitor of Differentiation 3 (Id3) attenuates high fat diet-induced obesity, but it is unclear if Id3 plays a role in diet-induced MCP-1 production. We sought to determine the initial cellular source of MCP-1 and identify molecular regulators mediating MCP-1 production.

Methods: $Id3^{+/+}$ and $Id3^{-/-}$ mice were fed either a standard chow or HFD for varying lengths of time. Flow cytometry, semi-quantitative real-time PCR, ELISAs and adoptive transfers were used to assess the importance of AdPCs during diet-induced obesity. Flow cytometry was also performed on a cohort of 14 patients undergoing bariatric surgery.

Results: Flow cytometry identified committed $CD45^-CD31^-Ter119^-CD29^+CD34^+Sca-1^+CD24^-$ adipocyte progenitor cells as producers of high levels of MCP-1 in VAT. High-fat diet increased AdPC numbers, an effect dependent on Id3. Loss of Id3 increased $p21^{Cip1}$ levels and attenuated AdPC proliferation, resulting in reduced MCP-1 and M1 macrophage accumulation in VAT, compared to $Id3^{+/+}$ littermate controls. AdPC rescue by adoptive transfer of 50,000 $Id3^{+/+}$ AdPCs into $Id3^{-/-}$ recipient mice increased MCP-1 levels and M1 macrophage number in VAT. Additionally, flow cytometry identified MCP-1-producing $CD45^-CD31^-CD34^+CD44^+CD90^+$ AdPCs in human omental and subcutaneous adipose tissue, with a higher percentage in omental adipose. Furthermore, high surface expression of CD44 marked abundant MCP-1 producers, only in visceral adipose tissue.

Conclusions: This study provides the first *in vivo* evidence, to our knowledge, that committed AdPCs in VAT are the initial source of obesity-induced MCP-1 and identifies the helix-loop-helix transcription factor Id3 as a critical regulator of $p21^{Cip1}$ expression, AdPC proliferation, MCP-1 expression and M1 macrophage accumulation in VAT. Inhibition of Id3 and AdPC expansion, as well as CD44 expression in human AdPCs, may serve as unique therapeutic targets for the regulation of adipose tissue inflammation.

1. INTRODUCTION

Chronic low-grade inflammation in visceral adipose tissue (VAT) links obesity to obesity-associated disease, such as cardiovascular disease, type II diabetes, and cancer [1,2]. Monocyte chemoattractant protein-1 (MCP-1) is a crucial mediator of chronic inflammation in VAT. Local and systemic levels of MCP-1 are increased in obese mice and humans compared to lean controls [3,4]. Increases in local production of MCP-1 in murine VAT can occur as early as 2 days post initiation of high-fat diet (HFD) [5]. These increased local levels of MCP-1 act as a chemotactic signal to recruit $CCR2^+$ proinflammatory monocytes that differentiate into $F4/80^+CD11c^+$ M1 macrophages upon entry into adipose tissue [6—8]. The increased ratio of proinflammatory M1 macrophages to resident $F4/80^+CD206^+$ M2 macrophages is a hallmark feature of

[1]Robert M. Berne Cardiovascular Research Center, University of Virginia, Charlottesville, VA, United States [2]Department of Pathology, University of Virginia, Charlottesville, VA, United States [3]Department of Biochemistry, Molecular Biology, and Genetics, University of Virginia, Charlottesville, VA, United States [4]Department of Surgery, University of Virginia, Charlottesville, VA, United States [5]Department of Medicine, Division of Cardiovascular Medicine, University of Virginia, Charlottesville, VA, United States [6]Beirne B. Carter Center for Immunology Research, University of Virginia, Charlottesville, VA, United States [7]Department of Molecular Physiology and Biological Physics, University of Virginia, Charlottesville, VA, United States

*Corresponding author. University of Virginia, PO Box 801394, 415 Lane Rd, Charlottesville, VA 22908, United States. Tel.: +1 434 243 8303; fax: +1 434 924 2828. E-mail: cam8c@virginia.edu (C.A. McNamara).

Original article

adipose tissue inflammation in murine visceral obesity [9], and links to metabolic disease through insulin resistance [10].

In sustained obesity, M1 macrophages become the main producers of MCP-1 and provide a positive feedback signal to recruit additional M1 macrophages [11]. However, M1 macrophages are not present in large numbers in murine adipose tissue until at least 8—10 weeks of HFD [12]. Obesity-induced production of MCP-1 occurs before these macrophages have migrated to the adipose tissue [13], suggesting that another cell type is responsible for early macrophage accumulation. Preliminary reports based on *in vitro* studies of preadipocyte cell lines and adherent SVF cells suggest that resident stromal cells express MCP-1 [14]. The stromal cell that initiates MCP-1-mediated macrophage accumulation in early obesity has not been clearly identified.

Recent work suggests that the transcription factor Inhibitor of Differentiation 3 (Id3) acts as a regulator of metabolic health in obesity [15,16]. Id3 is a dominant negative inhibitor of the basic helix-loop-helix (bHLH) family of transcription factors, which is a highly conserved group of proteins that play a role in the differentiation and growth of a variety of cell types [17,18]. Id3 decreases adiponectin transcription [19,20], promotes adipose tissue vascularization, and is necessary for diet-induced obesity [15,21]. Together, these data suggest that Id3 may play a key role in the early effects of diet-induced obesity. However, the role of Id3 *in vivo* in regulating MCP-1 production and early inflammatory mediators in obesity is unknown.

The present study is the first *in vivo* evidence, to our knowledge, that the source of early obesity-induced MCP-1 in VAT is adipocyte progenitor cells (AdPCs). Results demonstrated that as little as 1 week of HFD enhanced AdPC proliferation with resultant increase in local MCP-1 production. We identify Id3 as a critical regulator of p21^{Cip1} expression and proliferation in AdPCs. Consistent with these findings, mice null for Id3 had a loss of obesity-induced MCP-1 production. Importantly, adoptive transfer of $Id3^{+/+}$ AdPCs into $Id3^{-/-}$ mice significantly increased the amount of MCP-1 and the M1/M2 ratio in VAT. Lastly, we provide novel evidence that AdPCs in human VAT produce MCP-1, and identify CD44 as a key marker of MCP-1-producing AdPCs in human omental adipose.

2. MATERIALS AND METHODS

2.1. Mice

2.1.1. Breeding schema
The Institutional Animal Care and Use Committee of the University of Virginia have approved all animal experiments. Male mice on a *C57Bl/6J* background were used in all experiments. *C57Bl/6J* mice were purchased from Jackson Laboratory (stock# 000664). $Id3^{-/-}$ mice were provided by Yuan Zhuang (Duke University), and were bred with *C57Bl/6J* mice to generate $Id3^{+/-}$ mice that were used for breeding $Id3^{-/-}$ mice and $Id3^{+/+}$ littermate controls. $LysM^{cre/cre}$ mice were provided by Norbert Leitinger (University of Virginia). $Id3^{fl/fl}$ mice were provided by Yuan Zhuang (Duke University). $Id3^{fl/fl}$ mice were bred to $LysM^{cre/cre}$ mice to generate first $Id3^{fl/+}LysM^{cre/+}$ mice, which were bred to each other to generate $Id3^{fl/fl}LysM^{cre/+}$. These mice were then bred to $Id3^{fl/fl}LysM^{+/+}$ mice to generate $Id3^{fl/fl}LysM^{cre/+}$ and littermate control $Id3^{fl/fl}LysM^{+/+}$ mice. All mice, purchased or generated, were backcrossed at least 10 generations to *C57Bl/6J* mice. The number of mice used in each experiment is provided in the figure legends.

2.1.2. Diets
Mice were fed *ad libitum* with water and standard chow (Tekland 7012) or high-fat diet (60% fat, D12492, Research Diets) for the designated length of time.

2.2. Injections

2.2.1. BrdU injections
150 μl of BrdU (15 mg/ml, BD Biosciences) was intraperitoneally injected five times over the course of 1 week. Injections were at 72, 120, 144, 150 and 164 h post initiation of HFD.

2.2.2. Adoptive transfer injection
Donor $Id3^{-/-}$ and $Id3^{+/+}$ mice were fed a HFD for 2 weeks prior to transfer. 5.0×10^4 FACS-sorted (described below) CD45$^-$CD31$^-$Ter119$^-$CD29$^+$CD34$^+$Sca-1$^+$ adipocyte progenitor cells were intraperitoneally injected into $Id3^{-/-}$ hosts. Mice were given 3 days to recover before HFD was initiated.

2.3. Metabolic studies

2.3.1. Glucose tolerance test
Mice were fasted overnight in wood chip-lined cages. At the beginning of each experiment, a small tail snip was made and baseline blood glucose levels were determined. Mice were then injected i.p. with 1.4 g dextrose (Hospira) per kg body weight, and blood glucose levels were measured at 10, 20, 30, 60, 90, and 120 min post-injection. Mice had access to water *ad libitum* throughout the experiment.

2.3.2. Insulin injections for pAKT western
Mice were fasted overnight in wood chip-lined cages. Mice were injected with 10 U/kg insulin (Eli Lilly). Mice were euthanized after five minutes, and omental adipose tissue was removed and flash-frozen for later analysis (see Western blotting protocol below).

2.4. Tissue processing

2.4.1. Adipose tissue
Murine epididymal stroma-vascular fraction was isolated as previously described [15]. Human omental and subcutaneous adipose tissue was processed using published methods [22].

2.4.2. Peritoneal lavage
Peritoneal cells were harvested by peritoneal lavage 4 days after intraperitoneal injection of 3 ml of thioglycollate (BD Biosciences). Peritoneal macrophages were isolated by macs column purification with negative selection by CD4, CD8 and CD19 microbeads, followed by positive selection by F4/80 microbeads (Miltenyi Biotech).

2.4.3. PKH26 labeling
Isolated SVF cells were labeled with PKH26 (Sigma—Aldrich) according to manufacturer's instructions.

2.5. Flow cytometry
Red blood cells in the SVF were lysed if necessary with RBC lysis buffer (155 mM NH$_4$Cl, 10 mM KHCO$_3$, 0.1 mM Na$_2$EDTA, pH 7.4). All cells were strained through 70 μm filters and incubated with Fc-block (FCR-4G8, Invitrogen) for 10 min on ice prior to staining. Cells were stained on ice and protected from light for 20 min. Fc-block and antibodies were diluted in either FACS buffer (PBS containing 1% BSA and 0.05% NaN$_3$) for flow cytometry or sorting buffer (PBS containing 1% BSA) for cell sorting experiments. SVF cells were incubated with fluorophore-conjugated antibodies or fluorescent dyes for flow cytometry.

2.5.1. Murine flow cytometry antibodies
CD11c (N418), CD19 (1D3), CD24 (M1/69), CD29 (HMb1-1), CD3ε (500A2), F4/80 (BM8), and Sca-1 (D7) were purchased from

eBioscience, BrdU (B44), CD45 (30-F11), MCP-1 (2H5) and Ter119 (Ly-76) were purchased from BD Bioscience, CD206 (MMR), CD31 (390), and CD34 (MEC14.7) were purchased from BioLegend, and CD11b (M1/70.15) was purchased from Caltag.

2.5.2. Human flow cytometry antibodies
CD31 (WM59), CD34 (561), CD90 (5E10), CD44 (BJ18) were purchased from Biolegend and CD45 (2D1) was purchased from BD Bioscience.

Viability was determined by either LIVE/DEAD® fixable yellow cell staining (Invitrogen) or DAPI (Sigma−Aldrich). Cells were run on a CyAN ADP (Beckman Coulter) or sorted on an Influx Cell Sorter (Benton-Dickenson). Fluorescence minus one (FMO) samples were used to set gates for all antibodies. Flow cytometry was performed at the Flow Cytometry Core Facility at the University of Virginia. Cells were quantified using CountBright counting beads (Fisher). All flow cytometry data were analyzed using FlowJo 9.7.6 software (Tree Star Inc.).

2.5.3. Intracellular staining
Murine and human SVF cells were incubated for 5 h with Brefeldin A (Sigma−Aldrich), and cells were fixed and permeabilized with FIX&PERM (Invitrogen) according to manufacturer's instructions.

2.5.4. BrdU uptake
Cell proliferation was measured by the incorporation of BrdU into genomic DNA during the S phase of the cell cycle, using FITC BrdU Flow Kit (BDBiosciences).

2.5.5. FACS sorting
Murine AdPCs were sorted based on expression of CD29, CD34 and Sca-1, and were gated from cells negative for CD45, CD31, Ter119, and live/dead marker DAPI. Lineage positive (Lin+) cells were gated based on expression of CD45, CD31 or Ter119, and were gated from cells negative for live/dead marker DAPI. SVF cells were gated from cells negative for live/dead marker DAPI.

2.6. Promoter-reporter analysis
Full length Id3 was previously subcloned into a pAdlox expression vector [23]. p21Cip1 luciferase promoter construct [24] was a gift from Xiao-Hong Sun (Oklahoma University) and MCP-1 luciferase promoter construct was purchased from SwitchGear. 3T3-L1 and OP-9 cells were transfected with 0.9 μg of expression plasmid, using empty pAdlox vector to maintain the same amount of DNA, along with 0.1 μg of appropriate promoter. Twenty-four hours after transfection, luciferase activity was measured using the Luciferase Assay Kit (Promega) for p21Cip1 activity and LightSwitch Luciferase Assay Kit (SwitchGear) for MCP-1 activity, as per the manufacturer's instructions.

2.7. Cell and tissue culture
SVF cells, sorted primary cells, and whole adipose tissue were cultured in DMEM/F12-10, supplemented with 10% FBS and antibiotics. Media was collected after 24 h, and the supernatant was frozen in aliquots. Undifferentiated OP-9 cells and 3T3-L1 fibroblasts were maintained as previously described [19]. For adipogenesis, sorted primary adipocyte progenitor cells were cultured and induced to differentiate into adipocytes and stained with Oil Red O, as described elsewhere [25]. Transient transfections were performed three times in triplicate using FuGENE HD (Promega) according to the manufacturer's instructions. Empty vectors were used to keep the total DNA transfected uniform across all wells.

2.8. Real-time PCR
Total RNA was isolated from murine adipose tissue, isolated adipocytes, and SVF cells, reverse transcribed to cDNA, and used in real-time PCR reactions as described previously [19], with the following primers. Id3 forward TGCTACGAGGCGGTGTGCTG, reverse TGTCGTCCAAGAGGCTAAGAGGCT; p21Cip1 forward TCTCCCATTTCT-TAGTAGCAGTTG, reverse GCTTTGACACCCACGGTATT; MCP-1 forward GGTGTCCCAAAGAAGCTGTA, reverse TGTATGTCTGGACCCATTCC; Cyclophilin forward TGCCGGAGTCGACAATGAT, reverse TGGA-GAGCACCAAGACAGACA. All reactions were done in triplicate. The relative amount of all mRNAs was calculated using the comparative threshold cycle (C_t) method. Cyclophilin mRNA was used as the invariant control.

2.9. ELISA
MCP-1 ReadySetGo ELISA was performed on cell culture supernatant according to manufacturer's instructions (eBiosciences).

2.10. Study approval
Patients were recruited through the Bariatric Surgery Clinic at the University of Virginia. All patients were ≥18 years of age and obese (BMI ≥ 30), and provided informed written consent prior to participation in the study. The study was approved by the Human IRB Committee at the University of Virginia, IRB #14180. All procedures were in accord with the declaration of Helsinki.

2.11. Western blotting
Protein extracts from peritoneal macrophages and splenocytes, and western blotting were performed as previously described with antibodies against Id3 (Calbioreagents) and β-tubulin (Cell Signaling Technology). 10 (mg) omental adipose tissue was homogenized in 250ul protein lysis buffer (10% glycerol, 1% NP-40, 137 mM NaCl, 25 mM HEPES pH 7.4, 1 mM EGTA) containing protease inhibitors and phosphatase inhibitors (Sigma−Aldrich) and lysed on ice for 30 min. Protein lysate was collected and western blotting was performed with antibodies against AKT (1:1000, Cell Signaling) and Thr308 pAKT (1:1000, Cell Signaling), followed by horseradish peroxidase-linked secondary antibody (Jackson). Relative AKT phosphorylation was determined by normalizing pAKT to total AKT in each sample.

2.12. Statistics
All statistical analysis was performed using Prism 6.0a (GraphPad Software, Inc.). A two-tailed Student's t test was used to compare two independent, normally distributed groups and the Mann−Whitney test was used when one or more groups did not pass a Shapiro−Wilk normality test. Data are generally expressed as mean ± SEM. A p value < 0.05 was used to indicate significance, with non-significant data designated as ns.

3. RESULTS

3.1. CD45−CD34+ SVF cells are the predominant source of early HFD-induced MCP-1 production in VAT
To determine the main source of early HFD-induced MCP-1, isolated SVF cells and adipocytes from VAT of *C57Bl/6J* mice were analyzed for MCP-1 mRNA levels. There was significantly more MCP-1 mRNA in SVF cells in mice fed 1 week of HFD compared to chow-fed animals (Figure 1A). In contrast, the amount of mRNA in the adipocyte fraction did not significantly change (Figure 1B). In addition, the level of MCP-1 mRNA was higher in the SVF cells than in the adipocytes, from 1 week HFD-fed mice (Figure 1C). Consistent with this finding, analysis of the
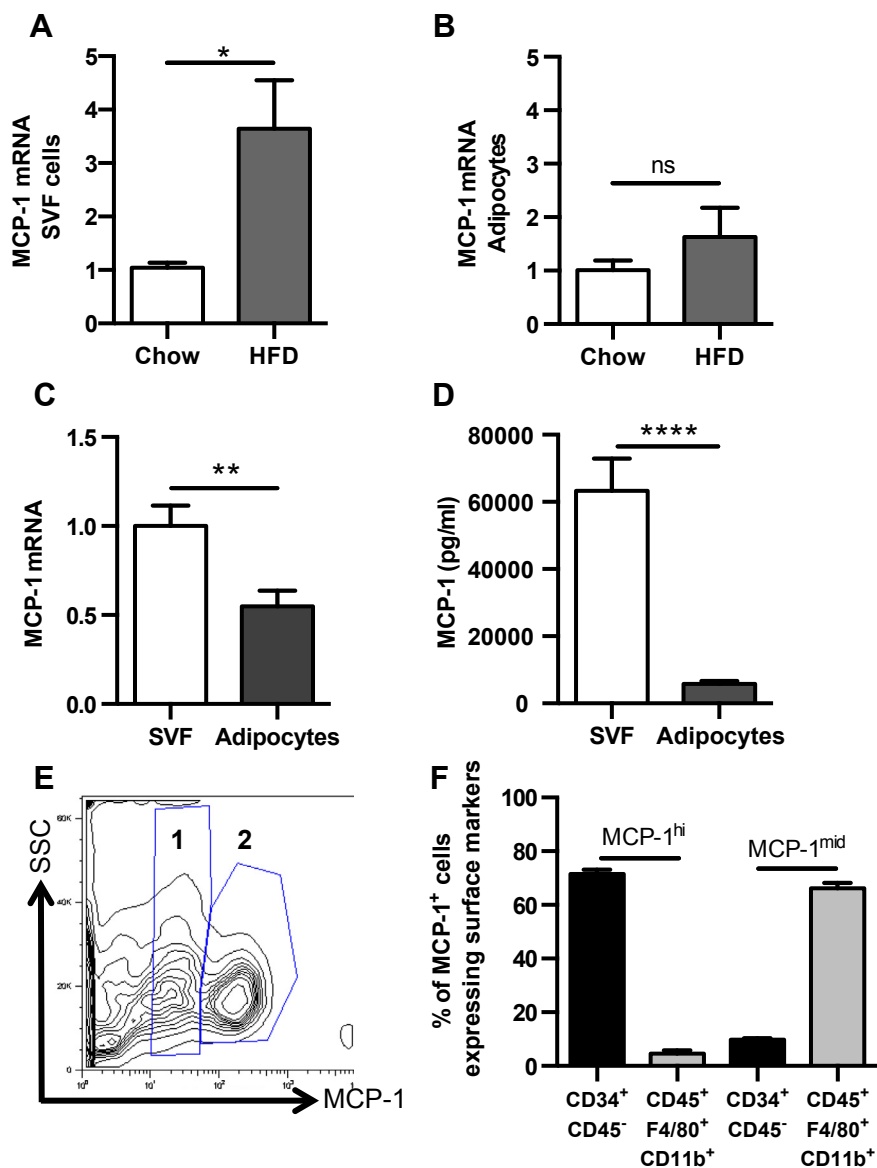
Figure 1: CD45⁻CD34⁺ SVF cells in VAT express high levels of MCP-1. (A–D) SVF and adipocytes were isolated from epididymal VAT of 8 to 10 week old *C57BL/6J* mice fed 1 week of either chow or HFD, and were analyzed for MCP-1 production. (A–C) MCP-1 mRNA levels in SVF cells and adipocytes, represented as fold increase over chow (A, B) and comparison between populations from HFD-fed mice (C). n = 10. (D) MCP-1 levels in the supernatant from SVF cells and adipocytes of 1 week HFD-fed *C57BL/6J* mice, cultured for 24 h n = 5. (E, F) Flow cytometry analysis of SVF cells from VAT of 8 to 10 week old *C57BL/6J* mice, n = 15. (E) Representative flow plot of intracellular MCP-1 staining in SVF. 1 = MCP-1^{mid}, 2 = MCP-1^{hi}. (F) Characterization of MCP-1^{hi} and MCP-1^{mid} cells using CD45, CD34, F4/80 and CD11b surface staining. 71.6 ± 1.5% of MCP-1^{hi} cells were CD45⁻CD34⁺ and 66.2 ± 2.1% of MCP-1^{mid} cells were CD45⁺F4/80⁺CD11b⁺. Shown are mean values ± SEM, *p < 0.05, **p < 0.01, ****p < 0.0001, ns = p > 0.05.

supernatant of isolated cultured SVF cells and adipocytes from mice fed 1 week of HFD demonstrated higher levels of MCP-1 secreted by SVF cells compared to adipocytes (Figure 1D).

To determine the initial SVF cell responsible for HFD-induced MCP-1 expression, intracellular MCP-1 staining via flow cytometry was performed on VAT from *C57Bl/6J* mice. Interestingly, two populations of MCP-1 positive cells were identified; those with low levels of fluorescence (MCP-1^{mid}) and those with high levels of fluorescence (MCP-1^{hi}) (Figure 1E). The gates were set based on the MCP-1 fluorescence-minus one (FMO) gate (Supplementary Figure 1A). The two populations, as well as the forward scatter/side scatter characteristics (Supplementary Figure 1B) suggested that more than one cell type within VAT was producing MCP-1, and that the level of expression was cell-type dependent. Utilizing cell surface markers to determine cell

phenotype, MCP-1^{hi} cells were identified as mostly CD45⁻CD34⁺, consistent with identification of a progenitor cell [26], although the type of progenitor cell could not be determined with this strategy. In contrast, the MCP-1^{mid} cells were mostly CD45⁺F4/80⁺CD11b⁺, consistent with a hematopoietic macrophage-like population [27] (Figure 1F).

3.2. Characterization of CD45⁻CD31⁻Ter119⁻CD29⁺CD34⁺Sca-1⁺ AdPCs

In the past several years, elegant methods to specifically identify adipocyte progenitor cells (AdPCs) using CD45⁻CD31⁻Ter119⁻CD29⁺CD34⁺Sca-1⁺ have become available [28]. Utilizing this gating strategy (Figure 2A), the two MCP-1-producing cell types were further characterized. To verify that these cells were AdPCs,

CD45$^-$CD31$^-$Ter119$^-$CD29$^+$CD34$^+$Sca-1$^+$ cells were sorted based on surface markers and cultured under adipogenic conditions. Consistent with previous findings [28], CD45$^-$CD31$^-$Ter119$^-$CD29$^+$CD34$^+$Sca-1$^+$ cells formed mature lipid-filled adipocytes as evidenced by morphology and Oil Red O staining (Supplementary Figure 1C, D).

To determine what percentage of this well-defined AdPC population produced high levels of MCP-1, intracellular staining for MCP-1 in combination with surface marker characterization to identify AdPCs, was performed. The vast majority of the MCP-1^{hi} cells were characterized as AdPCs based on surface marker expression (Figure 2B). Consistent with results in Figure 1F demonstrating that the MCP-1^{mid} cells were predominantly CD45$^+$F4/80$^+$CD11b$^+$, only a small percentage of the MCP-1^{mid} cells expressed AdPC surface markers (Figure 2B). To determine if the AdPCs with MCP-1^{hi} intracellular staining also secreted higher levels of MCP-1 compared to total SVF cells and lineage positive cells (Lin$^+$), equal numbers of each cell type sort-purified from VAT were cultured. Of note, AdPCs secreted the highest levels of MCP-1: twice as much as the total SVF, and about 10-fold more than the Lin$^+$ cells (Figure 2C).

AdPCs include cells at different stages of differentiation. CD24$^+$ AdPCs are upstream progenitor cells, and loss of CD24 expression occurs as they become further committed to the adipocyte lineage [29, 30]. To determine if there was a relationship between AdPC commitment and MCP-1 expression, MCP-1 intracellular staining was analyzed in both CD24$^+$ and CD24$^-$ AdPCs. Results demonstrated that it was the committed CD24$^-$ AdPCs that expressed high levels of MCP-1, while only a small percentage of upstream CD24$^+$ progenitors expressed MCP-1, as seen in the representative flow plot and quantitation of 15 mice (Figure 2D, E). Results suggested that further commitment to the adipocyte lineage stimulates AdPCs to produce high levels of MCP-1.

3.3. HFD induces proliferation of AdPCs

To determine the early effects of HFD on MCP-1 production by AdPCs, *C57Bl/6J* mice were fed HFD for 1 week. The numbers of MCP-1^{hi} and MCP-1^{mid} cells were quantified, and results demonstrated that HFD tripled the number of MCP-1^{hi} cells, while the number of MCP-1^{mid} cells was unchanged (Figure 3A). Since MCP-1^{hi} cells are primarily AdPCs, the number of AdPCs was also quantified in VAT after 1 week of HFD. Results demonstrated that 1 week of HFD doubled the number of AdPCs (Figure 3B), indicating that the increased number of MCP-1^{hi} cells may be due to an expansion of the pool of AdPCs.

To determine if HFD-increased AdPC numbers were due to HFD-induced proliferation, a bromodeoxyuridine (BrdU) uptake assay was
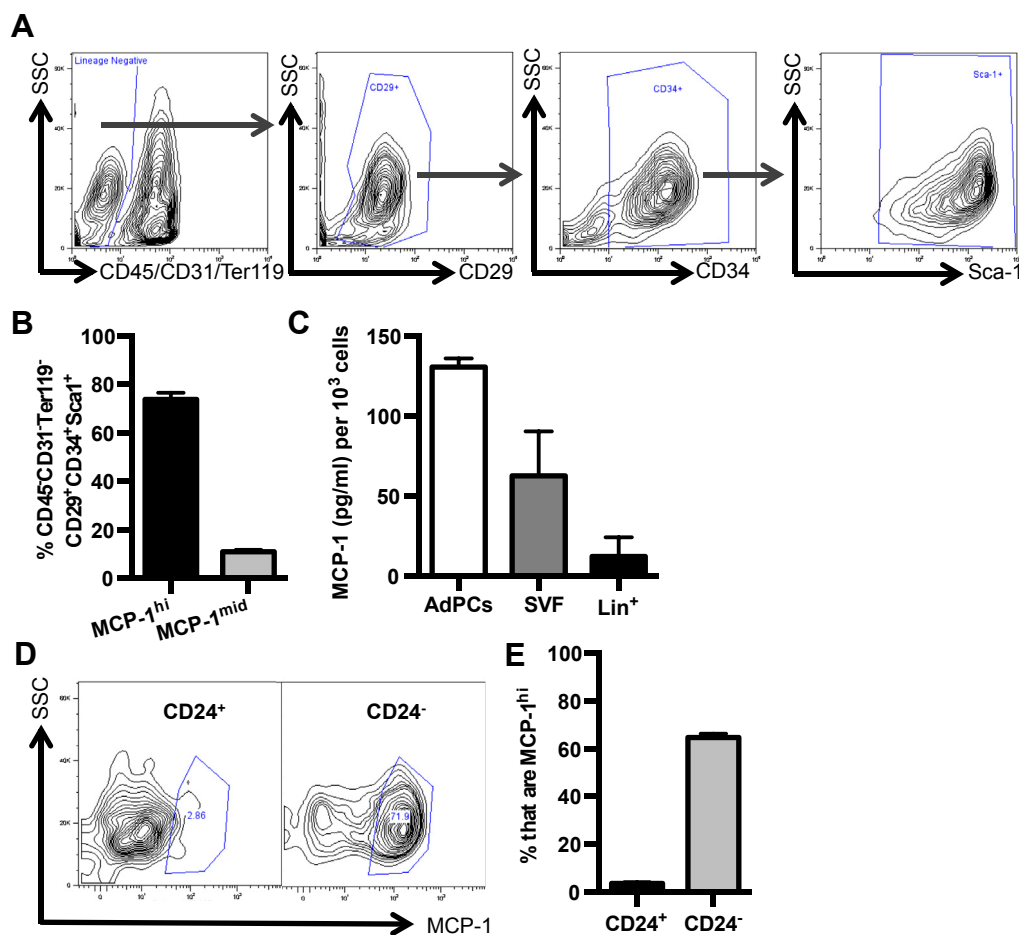

Figure 2: Committed CD45$^-$CD31$^-$CD29$^+$CD34$^+$Sca-1$^+$CD24$^-$ AdPCs express and secrete high levels of MCP-1. Epididymal VAT from 8 to 10 week old *C57BL/6J* mice was harvested and processed for SVF cells. (A, B) Flow cytometry analysis of CD45$^-$CD31$^-$Ter119$^-$CD29$^+$CD34$^+$Sca-1$^+$ AdPCs with representative flow plot (A) and the percentage (B) of AdPCs with MCP-1^{hi} and MCP-1^{mid} expression. n = 6 (C) MCP-1 levels as measured by ELISA in the supernatant of equivalent numbers of sort purified AdPCs, total SVF, and Lin$^+$ (CD45$^+$/CD31$^+$/Ter119$^+$) cells. n = 3, each group including 6—8 mice pooled. (D, E) Analysis of MCP-1^{hi} cells in CD24$^+$ and CD24$^-$ AdPCs with representative plots (D) and quantitation (E) of MCP-1 intracellular staining. n = 15. Shown are mean values ± SEM.
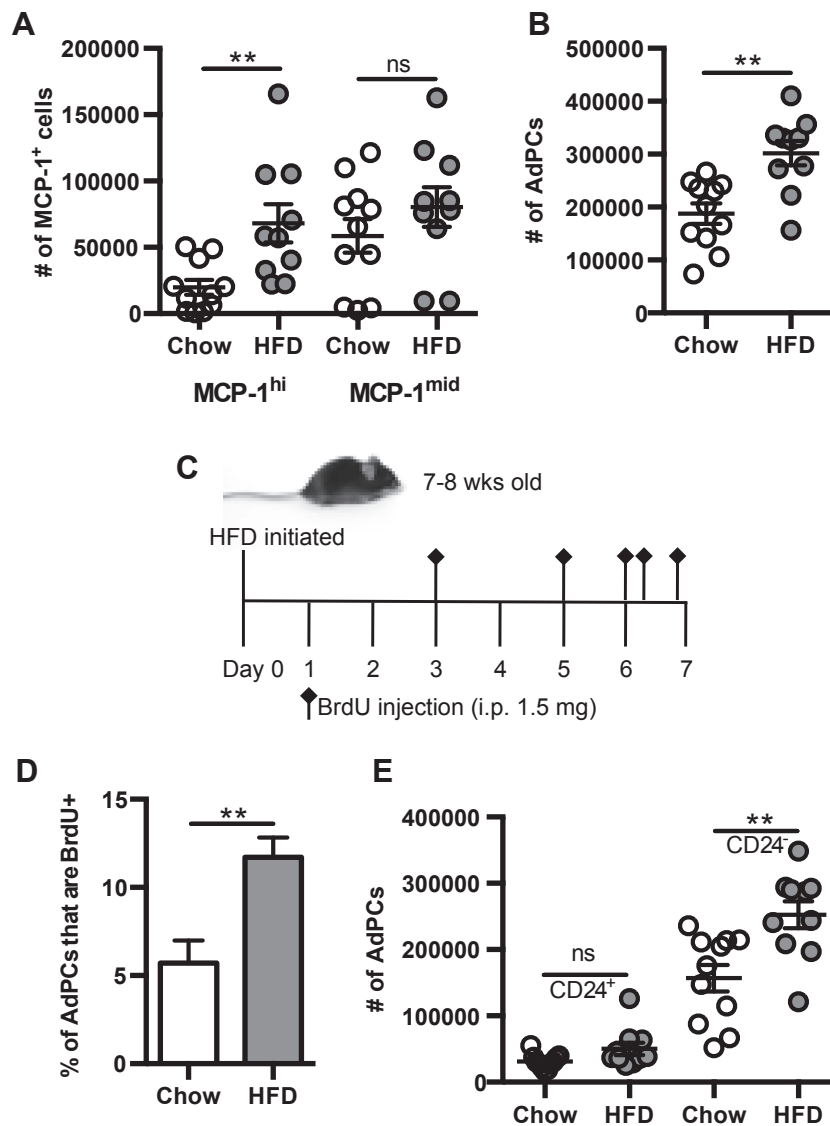
Figure 3: 1 week of HFD promotes proliferation of AdPCs. (A, B, E) SVF was isolated from epididymal VAT of 8 to 10 week old *C57BL/6J* mice fed 1 week of either chow or HFD. n = 10—11 per group. (A) Flow quantitation of MCP-1^{hi} and MCP-1[mid] cells per mouse (paired eVAT depots). (B) Flow quantitation of total AdPCs per mouse (paired eVAT depots). (C—D) 7 to 8 week old male *C57BL/6J* mice were fed standard chow or HFD for 1 week, and were injected with BrdU (bromodeoxyuridine) 5 times over the course of the diet. n = 11. (C) Time course of BrdU injections during 1 week of diet. (D) Percentage of BrdU uptake in AdPCs. (E) Flow quantitation of CD24^{+} and CD24^{−} AdPCs per mouse (paired eVAT depots). Shown are mean values ± SEM, **$p < 0.01$, ns = $p > 0.05$.

performed (Figure 3C). Results demonstrated a 2-fold increase in the percentage of AdPCs that incorporated BrdU into their DNA after 1 week of HFD (Figure 3D), indicating that proliferation was responsible for early increases in AdPC numbers. Of note, only CD24^{−} AdPCs expanded in response to HFD, while there was no change in the number of CD24^{+} AdPCs (Figure 3E). Thus, these data indicate that HFD results in an expansion of committed CD24^{−} adipocyte progenitor cells.

3.4. Id3 promotes HFD-induced proliferation of AdPCs through regulation of p21[Cip1]

To identify molecular mechanisms modulating HFD-induced AdPC proliferation, we utilized the *Id3*^{−/−} mouse. Id3 has been implicated in AdPC differentiation [20,31] and has known growth-promoting effects [23,32]. To determine first whether HFD led to changes in Id3 expression in AdPCs, Id3 mRNA levels were measured in sort-purified AdPCs from chow-fed and HFD-fed mice. Results demonstrated a

HFD-induced increase in Id3 expression in AdPCs (Figure 4A). To determine if loss of Id3 altered proliferation of AdPCs, BrdU uptake was measured in *Id3*^{−/−} mice and compared to *Id3*^{+/+} littermate controls. In contrast to *Id3*^{+/+} mice, *Id3*^{−/−} mice had no increase in proliferating AdPCs due to HFD (Figure 4B), providing evidence that HFD-induced proliferation of AdPCs is dependent on Id3.

To determine if loss in obesity-induced proliferation resulted in reduced CD24^{−} AdPCs in *Id3*^{−/−} mice, committed CD24^{−} AdPCs were quantified after 1 week of chow or HFD. In contrast to the *Id3*^{+/+} mice, the CD24^{−} AdPCs from *Id3*^{−/−} mice failed to expand after 1 week of HFD (Figure 4C). To confirm that the lack of increase in CD24^{−} AdPCs after HFD in the *Id3*^{−/−} mice was not due to an increase in adipocyte differentiation, Oil Red O uptake was measured. Consistent with previous findings [15], results demonstrated equivalent Oil Red O uptake between genotypes (Figure 4D), providing evidence that Id3 regulation of AdPC number is through proliferation and not differentiation.
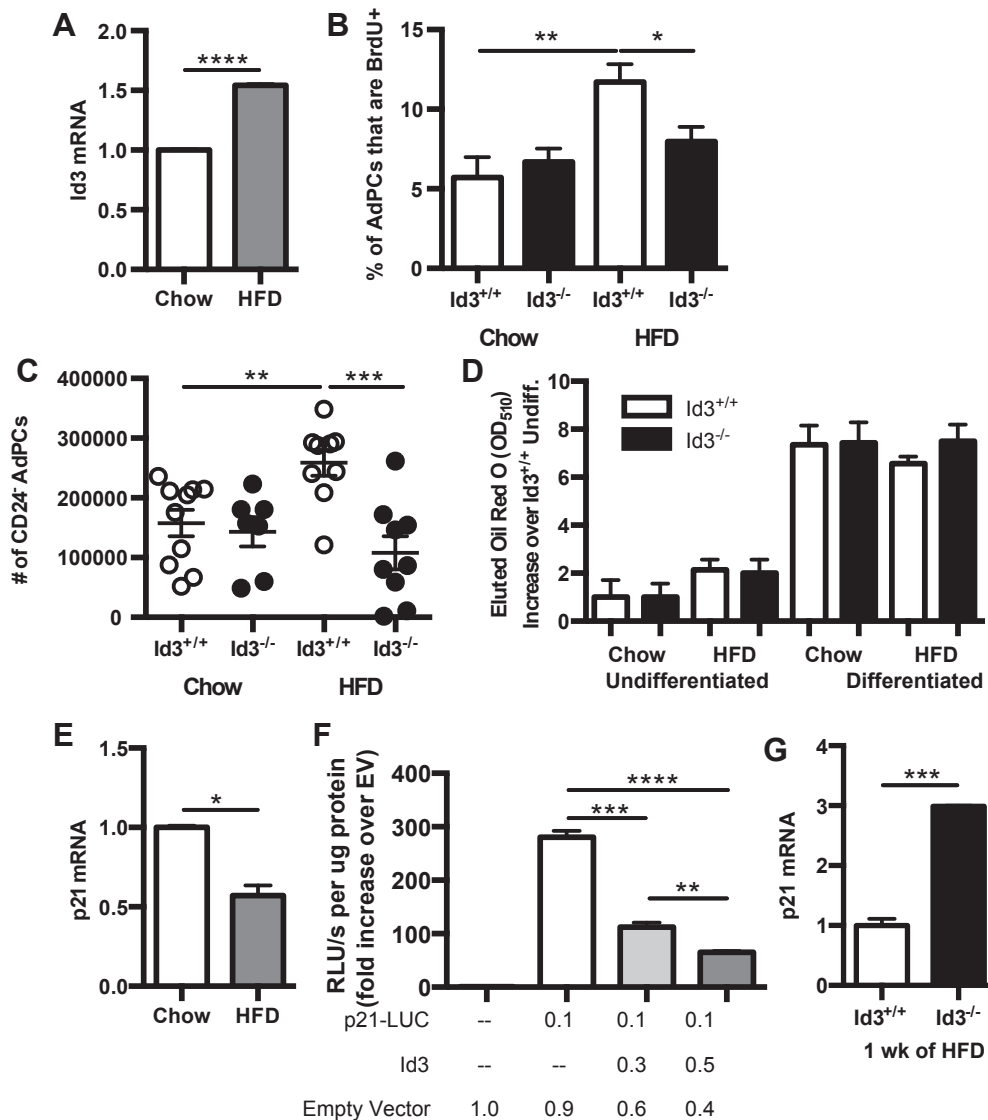
Figure 4: HFD reduces p21^{Cip1} expression and promotes proliferation of committed CD24$^-$ AdPCs in an Id3-dependent manner. (A, E) SVF was isolated from epididymal VAT of 8 to 10 week old *C57BL/6J* mice fed 1 week of either chow or HFD, and CD45$^-$CD31$^-$Ter119$^-$CD29$^+$CD34$^+$Sca-1$^+$ cells were sort purified. n = 3, each group including 6—8 mice pooled. (A) Id3 mRNA levels, represented as fold increase over chow. (B—D, G) SVF was isolated from epididymal VAT of 8 to 10 week old *Id3$^{+/+}$* and *Id3$^{-/-}$* mice fed 1 week of either chow or HFD. (B) Percentage of BrdU uptake in AdPCs, as described in Figure 3C. n = 7—11. (C) Quantitation of CD24$^-$ AdPCs per mouse (paired eVAT depots). n = 7—9. (D) Oil Red O staining from sort purified AdPCs cultured under adipogenic conditions. n = 3, each group including 6—8 pooled mice pooled. (E) p21^{Cip1} mRNA levels, represented as fold increase over chow. (F) p21^{Cip1} promoter activity in OP-9 cells, transfected with plasmid encoding ID3 and p21^{Cip1} luciferase-expressing promoter construct (p21-LUC), as measured by RLU (relative luminescence units). Performed in triplicate, repeated three times. (G) p21^{Cip1} mRNA expression, represented as fold increase over *Id3$^{+/+}$*. Shown are mean values ± SEM, *p < 0.05, **p < 0.01, ***p < 0.001, ****p < 0.0001.

Id3 has previously been demonstrated to inhibit the expression of p21^{Cip1} [18,32], a cyclin-dependent kinase inhibitor that prevents entrance into S phase, keeping cells growth-arrested in G1 [33]. To determine if HFD inhibits p21^{Cip1} expression in AdPCs, thereby promoting proliferation, p21^{Cip1} mRNA levels were measured in sort-purified AdPCs from chow-fed and HFD-fed mice. Results showed a significant decrease in p21^{Cip1} expression in AdPCs from mice fed HFD (Figure 4E). To determine if Id3 regulates p21^{Cip1} promoter activation in AdPCs, an Id3 expression construct was co-transfected with a p21^{Cip1} luciferase-expressing promoter construct into OP-9 and 3T3-L1 pre-adipocyte cell lines. Promoter reporter assays demonstrated that Id3 repressed p21^{Cip1} promoter activation in a dose-dependent manner in both OP-9 (Figure 4F) and 3T3-L1 cells (data not shown). In addition,

p21^{Cip1} mRNA levels were measured in AdPCs from both *Id3$^{-/-}$* mice and wild-type littermate controls. AdPCs from mice null for Id3 had significantly greater p21^{Cip1} mRNA levels (Figure 4G). These data together suggest that HFD-induced Id3 inhibits p21^{Cip1} expression and promotes cell cycle progression in AdPCs.

3.5. Id3 promotes adipose tissue MCP-1 levels through expansion of MCP-1^{hi} AdPCs

To determine if loss of Id3 attenuates the HFD-induced increase in MCP-1^{hi} cells, intracellular staining for MCP-1 was performed in *Id3$^{-/-}$* mice compared to *Id3$^{+/+}$* littermate controls. Results demonstrated a significant attenuation of obesity-induced MCP-1^{hi} cells in *Id3$^{-/-}$* mice (Figure 5A). As with the *Id3$^{+/+}$* mice, HFD did not change the
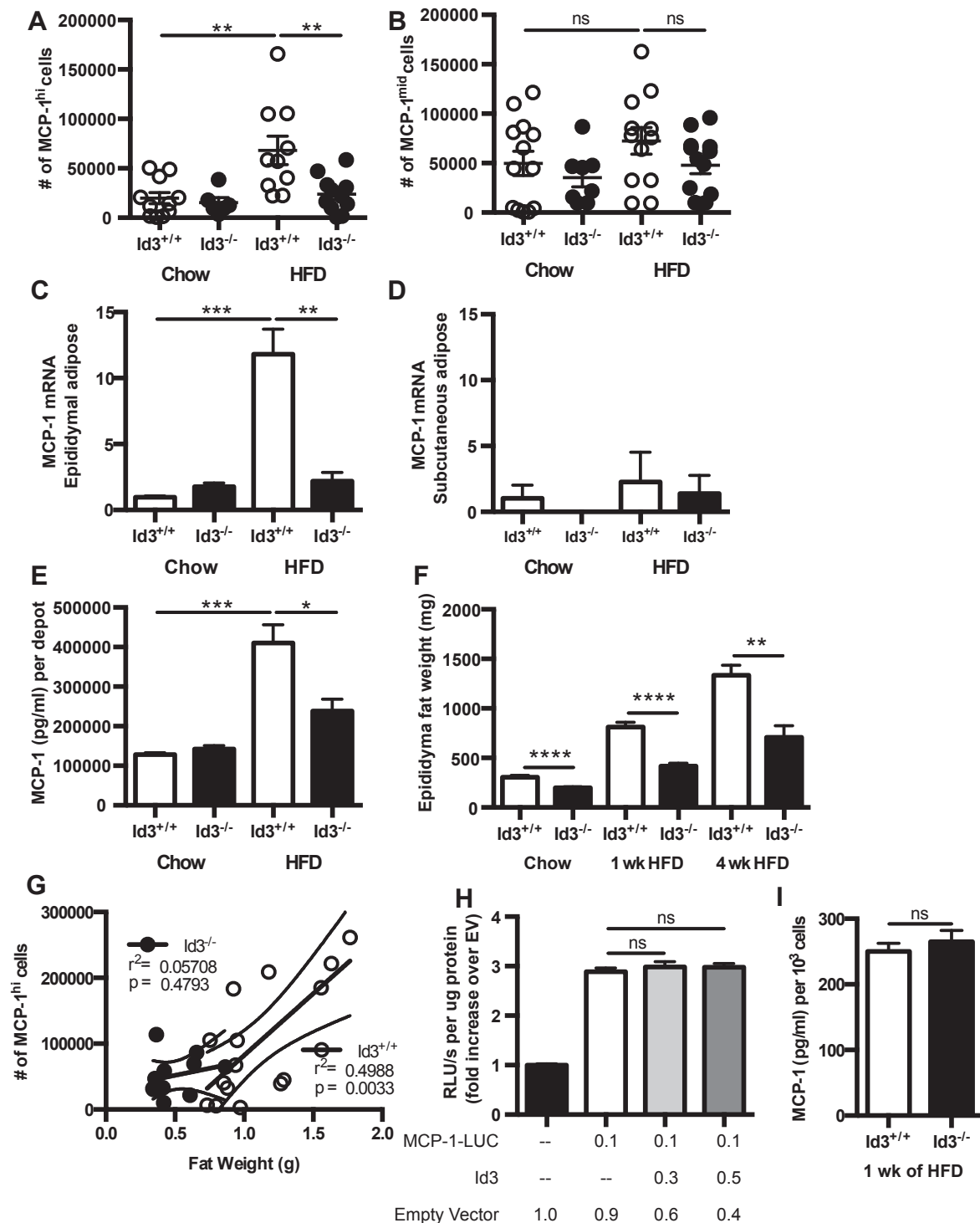
Figure 5: Id3 promotes HFD-induced MCP-1 in VAT. (A, B, G) SVF was isolated from epididymal VAT of 8 to 10 week old $Id3^{+/+}$ and $Id3^{-/-}$ mice fed 1 week of either chow or HFD. n = 7–10. Flow quantitation of MCP-1^{hi} cells (A) and MCP-1^{mid} cells (B) per mouse (paired eVAT depots). (C–E) Epididymal VAT and subcutaneous adipose tissue were harvested from 8 to 10 week old $Id3^{+/+}$ and $Id3^{-/-}$ mice fed 4 weeks of either chow or HFD. n = 5–6. (C, D) MCP-1 mRNA levels in epididymal (C) and subcutaneous (D) adipose, represented as fold increase over $Id3^{+/+}$ chow. (E) MCP-1 levels as measured by ELISA in the supernatant of epididymal VAT, cultured for 24 h. MCP-1 secretion was normalized per mouse (paired eVAT depots). (F) Weights of epididymal VAT from 8 to 10 week old $Id3^{+/+}$ and $Id3^{-/-}$ mice fed chow-diet or 1 or 4 weeks of HFD. (G) Correlation of quantified MCP-1^{hi} cells with epididymal VAT weight in 1 week HFD-fed $Id3^{+/+}$ and $Id3^{-/-}$ mice. (H) MCP-1 promoter activity in OP-9 cells, transfected with plasmid encoding ID3 and MCP-1 luciferase-expressing promoter construct (MCP-1-LUC), as measured by RLU (relative luminescence units). Performed in triplicate, repeated three times. (I) MCP-1 levels as measured by ELISA in the supernatant of sort purified AdPCs from 1 week HFD-fed mice. n = 3, each group including 6–8 pooled mice pooled. Shown are mean values ± SEM, *p < 0.05, **p < 0.01, ***p < 0.001, ****p < 0.0001, ns = p > 0.05.

number of MCP-1^{mid} cells in $Id3^{-/-}$ mice, and there was no difference due to loss of Id3 (Figure 5B). To determine if Id3 specifically promotes VAT MCP-1 expression and if early effects impact whole tissue at later time points, MCP-1 mRNA and protein levels were measured in both visceral and subcutaneous adipose tissue from $Id3^{+/+}$ and $Id3^{-/-}$ mice. $Id3^{+/+}$ mice had a significant increase in MCP-1 mRNA levels in VAT after 4 weeks of HFD, while this was markedly attenuated in mice null for Id3 (Figure 5C). This finding was specific to VAT, since there was no induction of MCP-1 mRNA levels in subcutaneous adipose tissue, nor were there Id3-dependent differences (Figure 5D). Consistent with the mRNA data, HFD-induced MCP-1 secretion from cultured VAT was attenuated in $Id3^{-/-}$ mice (Figure 5E). These data suggest that obesity-induced MCP-1 production in VAT is Id3-dependent.

To determine if Id3 regulates HFD-induced MCP-1 expression or secretion from adipocytes, adipocytes were isolated from $Id3^{+/+}$ and $Id3^{-/-}$ mice fed 1 week of HFD. Results demonstrated that there was no difference in either MCP-1 mRNA levels in the adipocytes due to global loss of Id3 (Supplementary Figure 2A). Isolated adipocytes were cultured for 24 h, and there was no difference in secretion from culture supernatant between groups (Supplementary Figure 2B).

As we have previously published that $Id3^{-/-}$ mice are partially protected from diet-induced obesity, we wanted to determine if reduced MCP-1 production in $Id3^{-/-}$ mice was accompanied by reduced adipose tissue expansion after 1 and 4 weeks of HFD. Indeed, while HFD induced an increase in epididymal VAT weight in both genotypes, $Id3^{-/-}$ mice had an attenuated effect (Figure 5F). Interestingly, while the number of MCP-1^{hi} cells found in VAT from $Id3^{+/+}$ mice correlated with the size of the fat depot, there was no such correlation in $Id3^{-/-}$ mice (Figure 5G), suggesting that the number of MCP-1^{hi} cells is not influenced by VAT depot size in these mice.

To determine if Id3 regulates MCP-1 gene expression and protein production on a per cell basis, promoter reporter and MCP-1 protein assays were performed. OP-9 and 3T3-L1 preadipocyte cell lines were co-transfected with an MCP-1 promoter luciferase reporter construct and a plasmid encoding Id3. Results demonstrated that Id3 had no effect on MCP-1 promoter activation (Figure 5H and data not shown). Equivalent numbers of sort purified AdPCs from $Id3^{-/-}$ mice and $Id3^{+/+}$ littermate controls were cultured and the supernatant was assayed for MCP-1. Results demonstrated no genotype-dependent differences in the level of MCP-1 produced (Figure 5I).

3.6. Id3 does not regulate MCP-1 in myeloid cells
Macrophages are important producers of MCP-1 [34]. To determine if loss of Id3 in macrophages affects MCP-1 expression, heterozygous transgenic mice containing Cre driven by the lysozyme promoter ($LysM^{Cre/+}$) were crossed with homozygous floxed Id3 mice ($Id3^{fl/fl}$) (Supplementary Figure 3A). The resultant $Id3^{fl/fl}LysM^{Cre/+}$ mice were null for $Id3$ specifically in myeloid cells, while myeloid cells from $Id3^{fl/fl}LysM^{+/+}$ littermates maintained Id3 expression. Deletion was confirmed in peritoneal macrophages (Supplementary Figure 3B, C). Myeloid-specific loss of Id3 did not affect HFD-induced MCP-1 secretion from VAT (Supplementary Figure 3D), providing evidence that Id3 is not regulating obesity-induced MCP-1 expression through a myeloid cell.

3.7. $Id3^{-/-}$ mice have reduced inflammatory macrophage content in VAT
MCP-1 has been shown to promote macrophage infiltration into adipose tissue, and $Id3^{-/-}$ mice have a significant reduction in MCP-1. To determine whether loss of Id3 attenuates HFD-induced

macrophage accumulation, flow cytometry was performed on VAT of $Id3^{+/+}$ and $Id3^{-/-}$ mice after 4 weeks of HFD. Results demonstrated that $Id3^{+/+}$ mice had a 2—3 fold obesity-induced increase in both F4/80$^+$CD11c$^+$ M1 and F4/80$^+$CD11c$^-$ M2 macrophage subsets (Figure 6A, B). In contrast, $Id3^{-/-}$ mice lacked an obesity-induced increase in M1 macrophages, resulting in a significantly reduced M1:M2 ratio compared to $Id3^{+/+}$ mice (Figure 6C). There were no differences in either macrophage subset in chow-fed animals. To determine if the reduced M1:M2 ratio in HFD-fed $Id3^{-/-}$ mice was accompanied by improved metabolic function, a glucose tolerance test (GTT) was performed in $Id3^{+/+}$ and $Id3^{-/-}$ mice after 2 weeks and 6 weeks of HFD. $Id3^{-/-}$ mice had improved glucose clearance compared to $Id3^{+/+}$ mice, at both time points (Figure 6D—E, G—H). To determine if $Id3^{-/-}$ mice also had improved insulin signaling in adipose tissue, western blotting for both total and phosphorylated AKT was performed on isolated VAT after insulin injection. $Id3^{-/-}$ mice had higher relative levels of AKT phosphorylation (Figure 6F), suggesting an improvement in insulin signaling, as compared to the $Id3^{+/+}$ mice.

3.8. Adoptive transfer of $Id3^{+/+}$ AdPCs to $Id3^{-/-}$ mice enhances MCP-1 expression and M1 macrophage accumulation in VAT
To determine if rescue of the deficiency in AdPC number in $Id3^{-/-}$ mice increased VAT MCP-1 and M1 macrophage numbers, $Id3^{-/-}$ recipient mice were i.p. injected with 50,000 sorted AdPCs from $Id3^{+/+}$ mice or $Id3^{-/-}$ mice fed 2 weeks of HFD, or vehicle control, and were fed HFD for 8 weeks (Figure 7A). A pilot experiment was performed to track injected cells (Supplementary Figure 4A), and confirmed that injected cells did traffic to the VAT within 1 week of injection. To determine if injection of $Id3^{+/+}$ AdPCs to $Id3^{-/-}$ mice would lead to metabolic dysfunction, GTTs were performed after 2 and 6 weeks of HFD. Indeed, $Id3^{-/-}$ mice receiving $Id3^{+/+}$ AdPCs had reduced glucose clearance over time compared to mice receiving $Id3^{-/-}$ AdPCs and vehicle control (Figure 7B, C and Supplementary Figure 4B, C). Interestingly, injection of $Id3^{+/+}$ AdPCs led to enhanced weight gain (Figure 7D) and VAT expansion (Figure 7E) in the $Id3^{-/-}$ mice, compared to vehicle control and injection if $Id3^{-/-}$ AdPCs. Injection of $Id3^{+/+}$ AdPCs to $Id3^{-/-}$ mice increased levels of MCP-1 in supernatant from VAT culture compared to mice receiving $Id3^{-/-}$ AdPCs and vehicle control (Figure 7F). Moreover, injection of $Id3^{+/+}$ AdPCs resulted in increased F4/80$^+$CD11c$^+$CD206$^-$ M1 macrophages (Figure 7G), while numbers of F4/80$^+$CD11c$^-$CD206$^+$ M2 macrophages were unchanged (Figure 7H), significantly enhancing the M1:M2 ratio (Figure 7I). These data provide evidence that MCP-1-producing AdPCs are key mediators of obesity-induced M1 macrophage accumulation in VAT, and that expression of Id3 in the AdPCs is crucial for these effects.

3.9. MCP-1 expression in human omental AdPCs is marked by high levels of CD44
As results in murine studies do not always reflect human disease, we evaluated omental and subcutaneous adipose tissue from a cohort of 14 obese patients undergoing bariatric surgery to determine if adipocyte progenitors in human VAT also express MCP-1. Intracellular cytokine staining and cell phenotyping via flow cytometry with markers validated to identify AdPCs in humans [35,36] was performed in omental and subcutaneous adipose tissue. These markers identified CD45$^-$CD31$^-$CD34$^+$CD90$^+$CD44$^+$ human AdPCs, which have been validated as functional adipocyte precursors [35]. Representative flow cytometry plots of human AdPCs in both omental and subcutaneous adipose tissue are depicted in Supplementary Figure 5A, B.
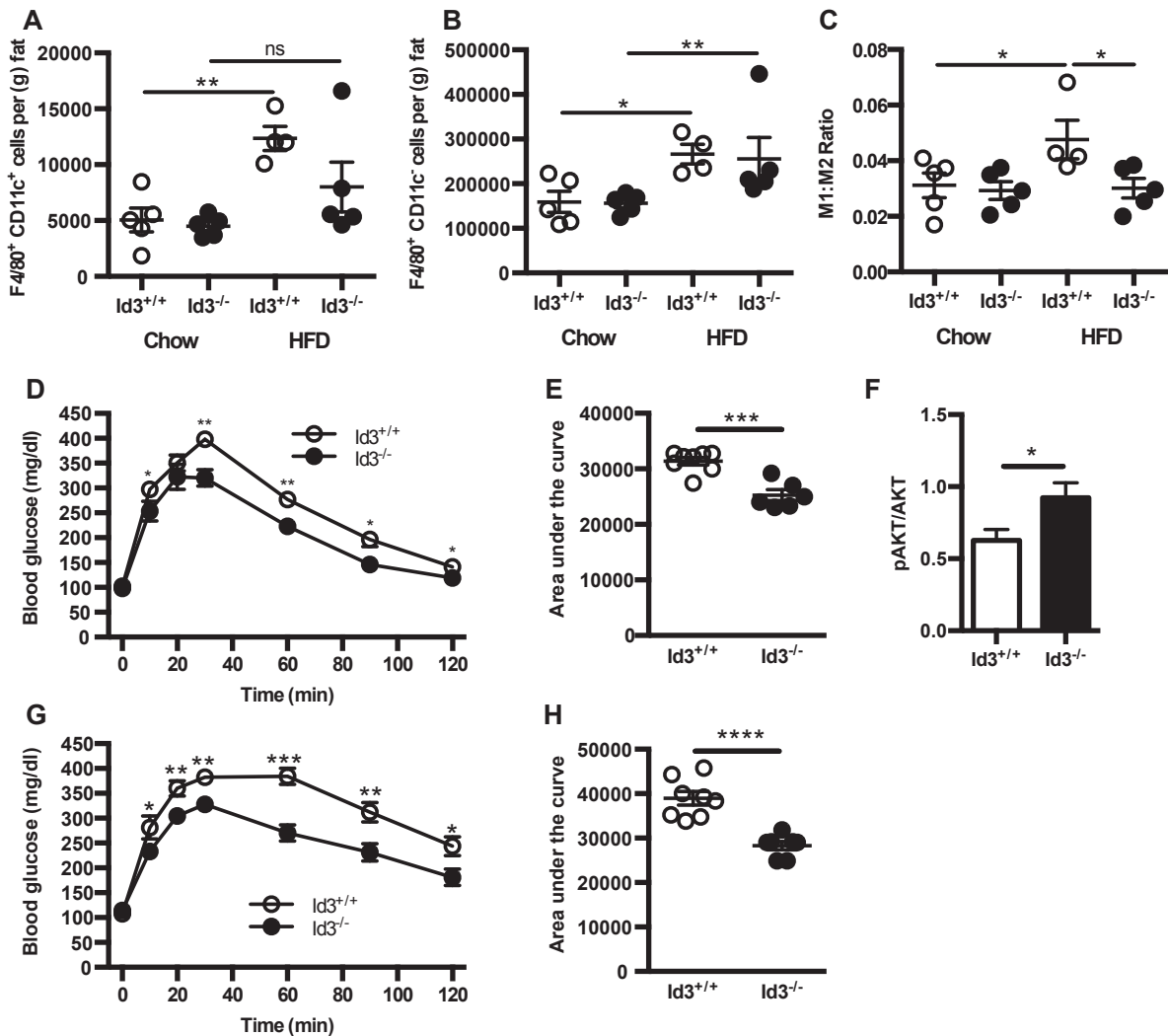
Figure 6: Loss of Id3 reduces HFD-induced VAT M1 macrophage accumulation (A—C) SVF was isolated from epididymal VAT of 8 to 10 week old *Id3*^{+/+} and *Id3*^{−/−} mice fed 4 weeks of either chow or HFD. n = 4—5. SVF cells were stained for flow cytometry quantitation of F4/80^{+}CD11c^{+} M1 macrophages (A), F4/80^{+}CD11c^{−} M2 macrophages (B) per gram of fat, and M1:M2 macrophage ratio (C). (D—F) 6 week-old *Id3*^{+/+} and *Id3*^{−/−} mice were fed 2 weeks of HFD. (D, E) Glucose tolerance test (GTT) was performed. n = 6—8. (D) Blood glucose measurements, with asterisks denoting comparison at individual time points. (E) Area under the curve measurements. (F) Western blotting for insulin-stimulated pAKT in omental adipose tissue, normalized to total AKT levels. n = 6—8. (G—H) 6 week-old *Id3*^{+/+} and *Id3*^{−/−} mice were fed 6 weeks of HFD. Glucose tolerance test (GTT) was performed. n = 6—8. (G) Blood glucose measurements, with asterisks denoting comparison at individual time points. (H) Area under the curve measurements. Shown are mean values ± SEM, *p < 0.05, **p < 0.01, ***p < 0.001, ****p < 0.0001, ns = p > 0.05.

Utilizing these surface markers, the percentage of SVF cells that were CD45^{−}CD31^{−}CD34^{+} CD90^{+}CD44^{+} AdPCs in both omental and subcutaneous adipose tissue was determined, finding similar percentages in both depots (Figure 8A). Intracellular staining for MCP-1 determined that a greater percentage of AdPCs from omental adipose were positive for MCP-1 than cells from subcutaneous adipose (Figure 8B and Supplementary Figure 5C, D). In addition, while most of the CD45^{−}CD31^{−} cells were positive for both CD34 and CD90, there appeared to be a broader range of CD44 expression within this progenitor cell population, particularly in omental adipose. Within the broad range of CD44 expression in omental AdPCs, the percentage of MCP-1^{+} cells greatly differed (Figure 8C). There was a larger percentage of MCP-1^{+} cells in the CD44^{hi} population than in the CD44^{lo} population (Figure 8D). Notably, in CD45^{−}CD31^{−}CD34^{+}CD90^{+} cells from omental adipose, the geometric mean fluorescence intensity (gMFI) of CD44 highly correlated to the gMFI of MCP-1 (Figure 8E). However, there was no correlation in subcutaneous adipose, nor was there a correlation in any other population of cells within the omental adipose (data not shown).

While CD44 was not one of the markers in the murine AdPC panel, the association of CD44 with MCP-1 production in humans led us to determine if CD44^{hi} AdPCs were also abundant producers of MCP-1 in mice. MCP-1 intracellular staining was analyzed in CD24^{−}CD44^{hi} AdPCs compared to CD24^{−}CD44^{lo} AdPCs. As seen in the human VAT, there was a larger percentage of MCP-1^{hi} cells in the CD44^{hi} population than in the CD44^{lo} population in both chow-fed and HFD-fed mice (Figure 8F). Additionally, in the CD24^{−} AdPCs, the gMFI of CD44 highly correlated to the gMFI of MCP-1, seen in both chow-fed and HFD-fed mice (Figure 8G). These data provide evidence that CD44 marks AdPCs that express the highest levels of MCP-1 both in mice and humans.
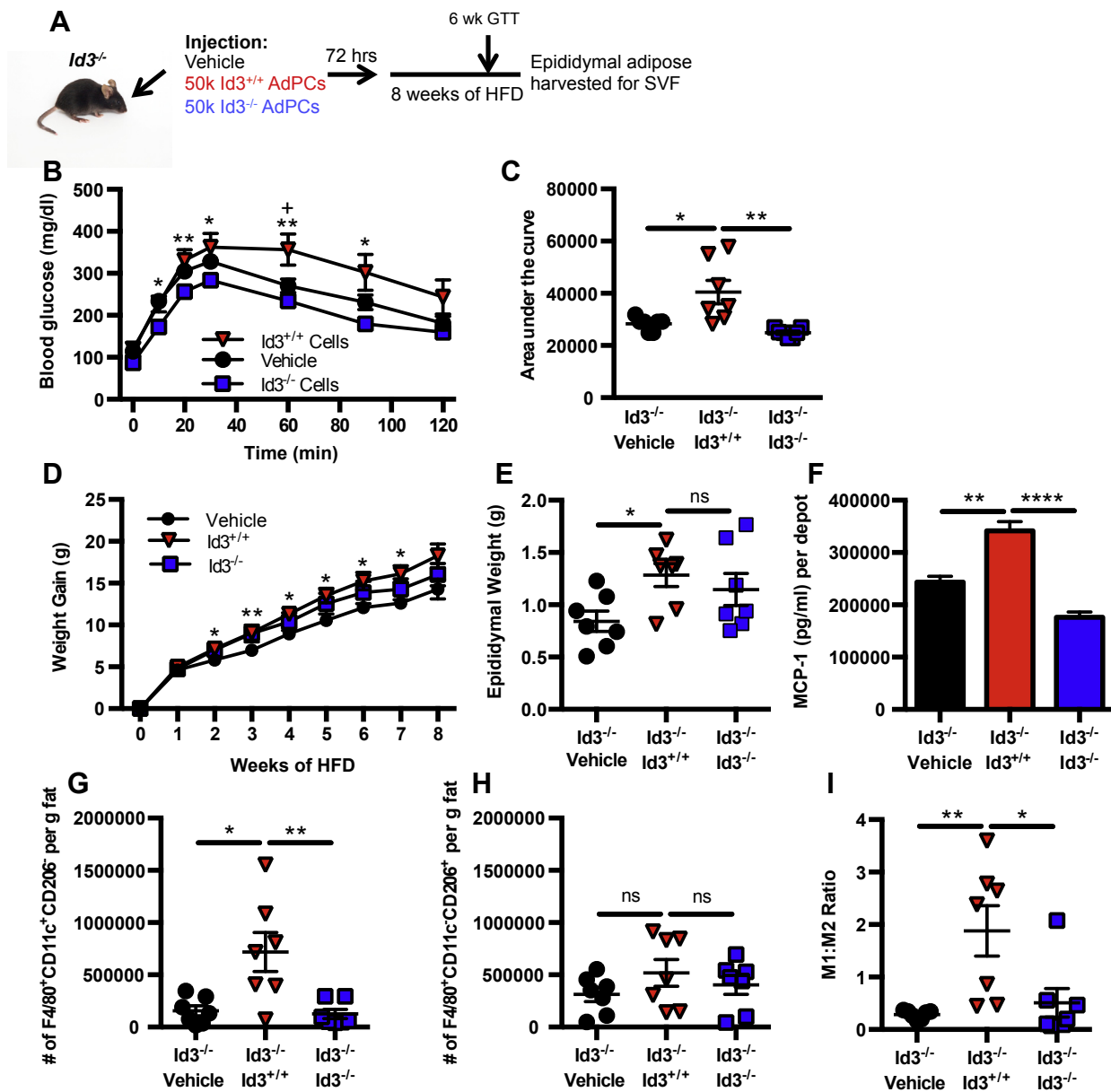
Figure 7: Adoptive transfer of _Id3_⁺/⁺ AdPCs restores HFD-induced MCP-1 expression and M1 macrophage accumulation in _Id3_⁻/⁻ mice (A) Setup of i.p. injection of vehicle or 50,000 sort-purified AdPCs from 2 week HFD-fed _Id3_⁺/⁺ mice or _Id3_⁻/⁻ mice into _Id3_⁻/⁻ recipient mice. n = 7. After 72 h, recipient mice were fed HFD. GTT was performed after 6 weeks of HFD, and mice were sacrificed after 8 weeks of HFD. (B–C) GTT performed after 6 weeks of HFD. (B) Blood glucose measurements, with asterisks denoting comparison at individual time points. + signifies comparison of vehicle to _Id3_⁺/⁺ cells and * signifies comparison of _Id3_⁺/⁺ cells to _Id3_⁻/⁻ cells (C) Area under the curve measurements. (D) Weight gain over 8 weeks of HFD, with asterisks denoting comparison of vehicle to _Id3_⁺/⁺ at individual time points. (E) Epididymal weights at sacrifice. (F) MCP-1 levels as measured by ELISA in the supernatant of epididymal VAT, cultured for 24 h. MCP-1 secretion was normalized per paired depots. (G–I) Flow quantitation of F4/80⁺CD11c⁺CD206⁻ M1 macrophages (G) and F4/80⁺CD11c⁻CD206⁺ M2 macrophages (H) per gram of fat and ratio of M1:M2 macrophages (I). Shown are mean values ± SEM, * or + p < 0.05, **p < 0.01, ****p < 0.0001, ns = p > 0.05.

4. DISCUSSION

The present study clearly identifies AdPCs as the initial source of MCP-1 in response to HFD in mice and demonstrates that AdPCs in humans also produce abundant MCP-1. Utilizing murine models, we demonstrate that the HFD-induced increase in MCP-1 is due to an increase in the number of MCP-1-producing AdPCs. We identify Id3 as a key mediator of HFD-induced AdPC proliferation, MCP-1 production and inflammatory macrophage accumulation in VAT.

MCP-1 is one of the most well characterized inflammatory factors produced during obesity because of its action as a potent chemo-attractant for M1 macrophages. When MCP-1 is deleted in mice, the number of M1 macrophages found in adipose tissue is significantly reduced [7]. Inhibition of M1 macrophage infiltration into adipose tissue leads to improvement of adipocyte function, as well as attenuation of obesity-induced insulin resistance [37]. While transcriptional regulation of MCP-1 has been very well characterized, the source of early obesity-induced MCP-1 is much less clear.
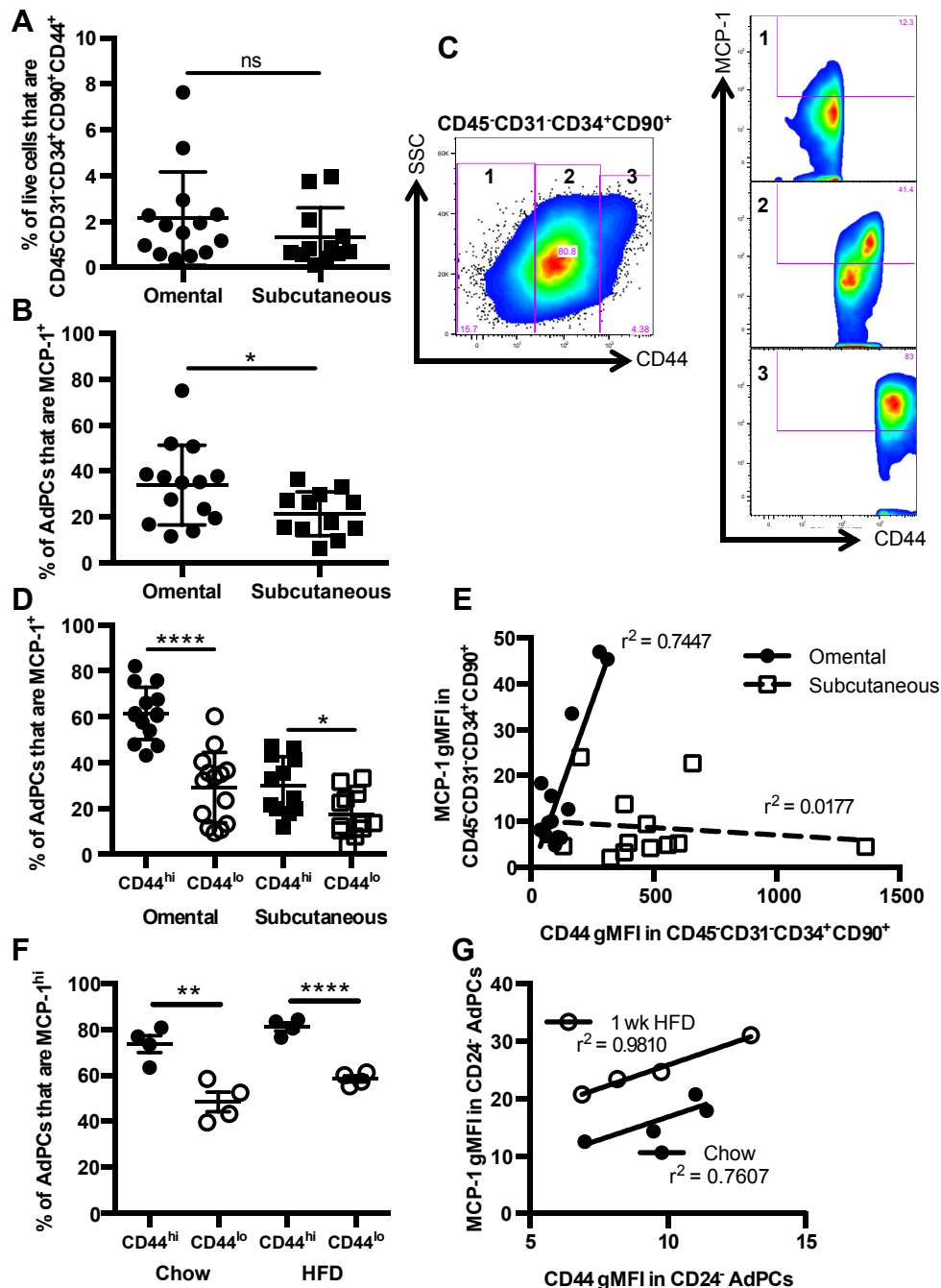
Figure 8: Human omental adipocyte progenitor cells express abundant MCP-1: an effect marked by high levels of CD44. (A–E) Subcutaneous and omental adipose tissue were collected during bariatric surgery from consenting human subjects (n = 14), and were processed to SVF cells for flow cytometry. (A) Percentage of SVF cells that were CD45$^-$CD31$^-$CD34$^+$CD90$^+$CD44$^+$ adipocyte progenitor cells in human omental and subcutaneous adipose tissue. (B) Percentage of AdPCs that were MCP-1$^+$ in omental and subcutaneous adipose tissue. (C) Representative plot depicting the heterogeneity of CD44 staining in CD45$^-$CD31$^-$CD34$^+$CD90$^+$ cells from omental VAT, and MCP-1 intracellular staining in each CD44 subset. 1 = CD44$^-$, 2 = CD44^{lo}, 3 = CD44^{hi} (D) Percentage of AdPCs that are MCP-1$^+$ as a function of CD44^{hi} and CD44^{lo} status in omental and subcutaneous adipose tissue. (E) Correlation of gMFI of MCP-1 with gMFI of CD44 in CD45$^-$CD31$^-$CD34$^+$ CD90$^+$ AdPCs in both omental and subcutaneous adipose tissue. Shown are mean values ± SD. (F, G) SVF was isolated from epididymal VAT of 8 to 10 week old *C57BL/6J* mice fed 1 week of either chow or HFD. n = 4. (F) Percentages of CD45$^-$CD31$^-$CD34$^+$CD29$^+$Sca-1$^+$CD24$^-$ AdPCs that are MCP-1^{hi} as a function of CD44^{hi} and CD44^{lo} status, in chow-fed and HFD-fed mice. (G) Correlation of gMFI of MCP-1 with gMFI of CD44 in CD45$^-$CD31$^-$CD34$^+$CD29$^+$Sca-1$^+$CD24$^-$ AdPCs, fed chow or HFD. Shown are mean values ± SEM, *p < 0.05, **p < 0.01, ****p < 0.0001, ns = p > 0.05. gMFI = Mean Fluorescence Intensity, using geometric mean.

Production of MCP-1 by adipocytes has been well documented [7,37], but evidence of higher production by SVF cells indicates that adipocytes are not the main source of MCP-1 during obesity [38]. The search for the cell that initially produces MCP-1 in response to HFD has implicated cells within the SVF, including endothelial cells [39], mast cells, and CD8$^+$ T cells [40]. This study provides clear *in vivo* evidence that AdPCs are the main sources of initial HFD-induced MCP-1 production.

Progenitor cells in tissues were originally thought to function as a reservoir of precursors poised to replenish the mature differentiated cells when needed. Yet, our data provide evidence of an important immunomodulatory function of AdPCs during times of altered tissue homeostasis as seen in disease states such as obesity, suggesting that progenitor cells have biological impact on the response to perturbation of homeostasis when in their undifferentiated state. This indicates that progenitor cells serve an additional function beyond replenishing the pool of differentiated cells.

It is well accepted that MCP-1 in adipose tissue functions to recruit inflammatory macrophages, promoting metabolic dysregulation during obesity. Indeed, our data implicate AdPC production of MCP-1 in M1 macrophage accumulation and glucose intolerance. However, it is intriguing to speculate as to why a progenitor cell would produce a macrophage chemoattractant when perturbed by nutritional access. As the adipose depot first starts to expand, macrophages recruited by MCP-1 may have multiple roles. An increase in blood supply is required to support the adipose tissue growth needed to accommodate the increased lipid with HFD. Macrophages support endothelial sprouting for the formation of new functional blood vessels [41], and Tie-2$^+$ angiogenic macrophages are recruited by MCP-1 [42]. Deletion of MCP-1 has been demonstrated to result in reduced tumor angiogenesis [43], suggesting that MCP-1 is important for new blood vessel formation to support rapidly expanding tissues. We have previously published that Id3 is an important regulator of HFD-induced visceral adipose expansion and microvascular blood volume [15]. While Id3 regulation of the expression of VEGFA a known angiogenic factor, was proposed as a potential mechanism mediating this effect, results of the present study raise the interesting possibility that loss of Id3 may also limit VAT microvascular blood volume and protect from HFD-induced VAT expansion by limiting AdPC proliferation and MCP-1 production. Adipocyte progenitors can reside in the adipose vasculature [44], as seen by expression of preadipocyte determination factor Zfp423 in capillary sprouts from human adipose tissue [45], allowing them to be conveniently poised to produce MCP-1 and attract the needed macrophages to support angiogenesis in the growing adipose depot. Further studies are needed to determine if AdPC-derived MCP-1 is necessary for VAT angiogenesis, although these studies will be challenging as there is no unique marker of AdPCs that can allow for AdPC-specific deletion of MCP-1.

The molecular pathways regulating normal adipose development during embryogenesis have been well described [46,47]. Yet, the molecular mechanisms mediating early AdPC expansion in response to HFD are incompletely understood. Recent evidence suggests that the serine threonine protein kinase AKT2 promotes early HFD-induced AdPC expansion in VAT, despite the fact that it is not essential for normal adipose development [48]. Similarly, necdin, a pleiotrophic protein that possesses pro-survival and anti-mitotic properties has been demonstrated to inhibit proliferation of adipocyte progenitors, but only in response to HFD [49]. Our murine studies provide evidence that the helix-loop-helix transcription regulator Id3 promotes HFD-induced AdPC accumulation in VAT. In similar fashion to AKT2 and necdin, Id3 does not affect normal adipose tissue growth and development, as adipose tissue size and body weight of $Id3^{-/-}$ mice match littermate $Id3^{+/+}$ controls at baseline [15]. Id3, normally expressed during development and in lymphocytes, can be re-expressed during disease [18] as seen previously in SVF from HFD-fed mice [15], and in results presented in this study. A role for Id3 in preadipocyte commitment and differentiation [31] has been suggested; however, results from the present study demonstrate that loss of Id3 has no effect on AdPC differentiation to adipocytes. Instead, results provide evidence that Id3

promotes HFD-induced AdPC proliferation in vivo. Furthermore, results suggest that it is this Id3-dependent AdPC expansion that is responsible for HFD-induced MCP-1 production, macrophage accumulation, and metabolic dysfunction.

We identify the cell cycle regulator p21^{Cip1} as a key Id3 target, possibly in HFD-induced AdPC proliferation. Loss of p21^{Cip1} has previously been demonstrated to attenuate HFD-induced adipocyte hyperplasia [50]. Consistent with these findings, 1 week of HFD significantly reduced p21^{Cip1} mRNA in AdPCs and mice null for Id3 have significantly more p21^{Cip1} mRNA in AdPCs in response to HFD, implicating Id3 and p21^{Cip1} as potential regulators of HFD-induced AdPC expansion.

While Id3 regulation of p21^{Cip1} in CD24$^-$ AdPCs may be one mechanism whereby Id3 regulates AdPC expansion, future studies involving loss and gain of p21^{Cip1} function are needed to confirm its essential role in HFD-induced AdPC expansion. Id3 may regulate AdPC numbers through other mechanisms besides proliferation. Furthermore, reduced MCP-1 production due to reduced numbers of AdPCs may not be the only mechanism whereby loss of Id3 attenuates macrophage numbers in adipose tissue and improves metabolic function. Results seen due to global loss of Id3, as well as after adoptive transfer of $Id3^{+/+}$ AdPCs into the Id3-deficient host were surprisingly dramatic, relative to changes in adipose tissue macrophage recruitment and metabolic function in mouse models with deletion of MCP-1 [7,51,52]. Id3 regulates many pathways, such as those involved in growth, differentiation, apoptosis, and chemokine and cytokine production. Further studies to identify additional mechanisms whereby Id3 in AdPCs regulates macrophage accumulation and glucose intolerance are ongoing. Id3 has previously been implicated in the role of adipose tissue expansion and HFD-induced weight gain [15]. One potential caveat to this study could be that effects seen here are simply secondary to the reduction in diet-induced obesity. However, $Id3^{-/-}$ mice do not have significant attenuation in HFD-induced total weight gain until 16 weeks of HFD [15]. Surprisingly, we did see reduced VAT mass in $Id3^{-/-}$ mice after 1 and 4 weeks of HFD. It is not yet clear if differences in MCP-1 are secondary to altered VAT expansion, or if increased MCP-1 in the $Id3^{+/+}$ mice is promoting weight gain. Additionally, while an expansion in fat mass of $Id3^{+/+}$ mice correlated with an increase in MCP-1^{hi} cells and AdPCs, there was no such correlation in $Id3^{-/-}$ mice, despite fat expansion (Figure 5G and data not shown). Importantly, as seen in the adoptive transfer experiment in Figure 7, $Id3^{-/-}$ mice receiving $Id3^{+/+}$ AdPCs had similar weights and adipose tissue expansion to those receiving $Id3^{-/-}$ AdPCs, but had altered M1:M2 ratio and worsened glucose metabolism. This indicates that the roles of Id3 and AdPCs extend beyond expansion of fat mass.

In the context of this study, we focused on the role of AdPC expansion and production of MCP-1, but it is clear that AdPCs are playing roles in addition to MCP-1-induced M1 macrophage accumulation.

MCP-1 is an important regulator of M1 macrophage accumulation in visceral adipose tissue, but it is of course not the only chemokine or cytokine involved in adipose tissue inflammation, and it is also not the only means to expansion of adipose tissue macrophages. Future studies identifying the initial source of other chemokines, and the role of AdPCs in producing these factors, would be of interest. The AdPCs could also be altering other populations within the adipose tissue, leading to the results that we have presented here. Future study of this unique population of cells is required to fully understand their role in diet-induced obesity.

Our murine results demonstrated significantly greater MCP-1 expression in the CD24$^-$ AdPCs compared to the CD24$^+$ AdPCs, suggesting that CD24 may inhibit AdPC production of MCP-1. Supporting this hypothesis, global deletion of CD24 results in rapid

increase in both local and systemic levels of MCP-1 in a murine cecal ligation and puncture model [53]. In addition to representing the commitment status of progenitor cells, CD24 is a glycosylphosphatidylinositol-anchored cell surface protein [54], also known as Heat Stable Antigen, with expression in a variety of cell types. Its function is poorly understood, owing to its variable glycosylation in different cell types [55] and its lack of a cytoplasmic domain, preventing intracellular signaling [56]. Whether CD24 expression in AdPCs is directly regulating MCP-1 production, or if it marks an adipocyte commitment step that promotes MCP-1 production, is unknown. Interestingly, CD24 is not used in the identification of human adipocyte progenitor cells, and it is not clear if its expression has different functions in murine versus human AdPCs.

Human AdPCs bear a unique set of identifying surface markers from mouse AdPCs, and are identified by lack of CD45 and CD31, and expression of CD34, CD44 and CD90 [35,57]. Utilizing these markers, we identified AdPCs in obese human omental and subcutaneous adipose tissue. Consistent with visceral adipose depots harboring more inflammation than subcutaneous adipose depots we found that AdPCs in human omental adipose produced more MCP-1 than cells from subcutaneous adipose. These data suggest that adipose depot-specific differences in inflammation may be due to depot-specific differences in AdPCs. Indeed, previous studies have suggested that AdPCs in the different depots arise from different precursor origins, and may not share a common precursor cell [58,59]. In addition, recent findings provide evidence that HFD-induced AdPC proliferation was limited to the VAT, and not seen in subcutaneous adipose [48]. This introduces the possibility that the greater inflammation seen in omental compared to subcutaneous adipose tissue may be due, at least in part, to greater production of MCP-1 by AdPCs. This may be quite relevant for human disease, as omental adipose tissue has been directly linked to metabolic disease and insulin resistance through MCP-1 production and macrophage infiltration [60].

Notably, results also demonstrated that CD44 marks a unique population of AdPCs that express abundant MCP-1 in VAT from both mice and humans. CD44 is a receptor for both osteopontin (OPN) and hyaluronic acid, and has been shown to upregulate overall MCP-1 levels via receptor engagement with these ligands [61–63]. Studies have demonstrated that levels of OPN [64] and hyaluronic acid [65] increase during obesity. CD44 levels in serum of obese human subjects positively correlated with the prevalence of insulin resistance, as well as to HbA1c, an index of glycemic control [66]. Direct targeting of CD44 in VAT AdPCs could provide a therapeutic strategy to potentially diminish adipose tissue inflammation.

The inflammation associated with obesity has been linked to diseases such as atherosclerosis [67], cancer [68], and autoimmune disease [69]. Efforts have been made to diminish systemic inflammation in the hope of treating obesity-related disease, as with anti-TNFα treatment. However, it was demonstrated that systemic ablation of this proinflammatory signaling pathway resulted in dysfunctional adipogenesis, hepatic steatosis, and ectopic lipid accumulation [70]. Learning more about the inflammatory properties of AdPCs could provide a unique approach to targeting harmful adipose tissue inflammation and obesity-associated disease, while preserving immune homeostasis. The novel demonstration of MCP-1-producing AdPCs in human omental adipose underscores the potential clinical relevance of these data as it opens the door for discovery of unique approaches that could lead to strategies that would limit the obesity-induced inflammatory cascade at an early stage, preventing the amplification of inflammation seen with the chronic accumulation of inflammatory macrophages.

CONFLICT OF INTEREST

None declared.

APPENDIX A.   SUPPLEMENTARY DATA

Supplementary data related to this article can be found at http://dx.doi.org/10.1016/j.molmet.2015.07.010.

REFERENCES

[1] Jia, H., Lubetkin, E.I., 2010. Trends in quality-adjusted life-years lost contributed by smoking and obesity. American Journal of Preventive Medicine 38:138–144.

[2] Kaminski, D.A., Randall, T.D., 2010. Adaptive immunity and adipose tissue biology. Trends in Immunology 31:384–390.

[3] Jiao, P., Chen, Q., Shah, S., Du, J., Tao, B., Tzameli, I., et al., 2009. Obesity-related upregulation of monocyte chemotactic factors in adipocytes: involvement of nuclear factor-kappaB and c-Jun NH2-terminal kinase pathways. Diabetes 58:104–115.

[4] Nomura, S., Shouzu, A., Omoto, S., Nishikawa, M., Fukuhara, S., 2000. Significance of chemokines and activated platelets in patients with diabetes. Clinical & Experimental Immunology 121:437–443.

[5] Chen, A., Mumick, S., Zhang, C., Lamb, J., Dai, H., Weingarth, D., et al., 2005. Diet induction of monocyte chemoattractant protein-1 and its impact on obesity. Obesity Research 13:1311–1320.

[6] Dalmas, E., Clement, K., Guerre-Millo, M., 2011. Defining macrophage phenotype and function in adipose tissue. Trends in Immunology 32:307–314.

[7] Kanda, H., Tateya, S., Tamori, Y., Kotani, K., Hiasa, K., Kitazawa, R., et al., 2006. MCP-1 contributes to macrophage infiltration into adipose tissue, insulin resistance, and hepatic steatosis in obesity. Journal of Clinical Investigation 116:1494–1505.

[8] Singer, K., DelProposto, J., Morris, D.L., Zamarron, B., Mergian, T., Maley, N., et al., 2014. Diet-induced obesity promotes myelopoiesis in hematopoietic stem cells. Molecular Metabolism 3:664–675.

[9] Fujisaka, S., Usui, I., Bukhari, A., Ikutani, M., Oya, T., Kanatani, Y., et al., 2009. Regulatory mechanisms for adipose tissue M1 and M2 macrophages in diet-induced obese mice. Diabetes 58:2574–2582.

[10] Lumeng, C.N., Bodzin, J.L., Saltiel, A.R., 2007. Obesity induces a phenotypic switch in adipose tissue macrophage polarization. Journal of Clinical Investigation 117:175–184.

[11] Coenen, K.R., Gruen, M.L., Chait, A., Hasty, A.H., 2007. Diet-induced increases in adiposity, but not plasma lipids, promote macrophage infiltration into white adipose tissue. Diabetes 56:564–573.

[12] Kintscher, U., Hartge, M., Hess, K., Foryst-Ludwig, A., Clemenz, M., Wabitsch, M., et al., 2008. T-lymphocyte infiltration in visceral adipose tissue: a primary event in adipose tissue inflammation and the development of obesity-mediated insulin resistance. Arteriosclerosis, Thrombosis and Vascular Biology 28:1304—1310.

[13] Nguyen, M.T., Favelyukis, S., Nguyen, A.K., Reichart, D., Scott, P.A., Jenn, A., et al., 2007. A subpopulation of macrophages infiltrates hypertrophic adipose tissue and is activated by free fatty acids via Toll-like receptors 2 and 4 and JNK-dependent pathways. Journal of Biological Chemistry 282:35279—35292.

[14] Gao, D., Trayhurn, P., Bing, C., 2013. 1,25-Dihydroxyvitamin D3 inhibits the cytokine-induced secretion of MCP-1 and reduces monocyte recruitment by human preadipocytes. International Journal of Obesity (London) 37:357—365.

[15] Cutchins, A., Harmon, D.B., Kirby, J.L., Doran, A.C., Oldham, S.N., Skaflen, M., et al., 2012. Inhibitor of differentiation-3 mediates high fat diet-induced visceral fat expansion. Arteriosclerosis, Thrombosis and Vascular Biology 32:317—324.

[16] Svendstrup, M., Vestergaard, H., 2014. The potential role of inhibitor of differentiation-3 in human adipose tissue remodeling and metabolic health. Molecular Genetics and Metabolism 113:149—154.

[17] Benezra, R., Davis, R.L., Lockshon, D., Turner, D.L., Weintraub, H., 1990. The protein Id: a negative regulator of helix-loop-helix DNA binding proteins. Cell 61:49—59.

[18] Ruzinova, M.B., Benezra, R., 2003. Id proteins in development, cell cycle and cancer. Trends in Cell Biology 13:410—418.

[19] Doran, A.C., Meller, N., Cutchins, A., Deliri, H., Slayton, R.P., Oldham, S.N., et al., 2008. The helix-loop-helix factors Id3 and E47 are novel regulators of adiponectin. Circulation Research 103:624—634.

[20] Moldes, M., Boizard, M., Liepvre, X.L., Feve, B., Dugail, I., Pairault, J., 1999. Functional antagonism between inhibitor of DNA binding (Id) and adipocyte determination and differentiation factor 1/sterol regulatory element-binding protein-1c (ADD1/SREBP-1c) trans-factors for the regulation of fatty acid synthase promoter in adipocytes. Biochemical Journal 344(Pt 3):873—880.

[21] Das, J.K., Felty, Q., 2014. PCB153-induced overexpression of ID3 contributes to the development of microvascular lesions. PLoS One 9:e104159.

[22] Zimmerlin, L., Donnenberg, V.S., Donnenberg, A.D., 2011. Rare event detection and analysis in flow cytometry: bone marrow mesenchymal stem cells, breast cancer stem/progenitor cells in malignant effusions, and pericytes in disaggregated adipose tissue. Methods in Molecular Biology 699:251—273.

[23] Forrest, S.T., Taylor, A.M., Sarembock, I.J., Perlegas, D., McNamara, C.A., 2004. Phosphorylation regulates Id3 function in vascular smooth muscle cells. Circulation Research 95:557—559.

[24] Prabhu, S., Ignatova, A., Park, S.T., Sun, X.H., 1997. Regulation of the expression of cyclin-dependent kinase inhibitor p21 by E2A and Id proteins. Molecular Cell Biology 17:5888—5896.

[25] Church, C.D., Berry, R., Rodeheffer, M.S., 2014. Isolation and study of adipocyte precursors. Methods in Enzymology 537:31—46.

[26] Stella, C.C., Cazzola, M., De Fabritiis, P., De Vincentiis, A., Gianni, A.M., Lanza, F., et al., 1995. CD34-positive cells: biology and clinical relevance. Haematologica 80:367—387.

[27] Davies, L.C., Jenkins, S.J., Allen, J.E., Taylor, P.R., 2013. Tissue-resident macrophages. Nature Immunology 14:986—995.

[28] Rodeheffer, M.S., Birsoy, K., Friedman, J.M., 2008. Identification of white adipocyte progenitor cells in vivo. Cell 135:240—249.

[29] Berry, R., Rodeheffer, M.S., 2013. Characterization of the adipocyte cellular lineage in vivo. Nature Cell Biology 15:302—308.

[30] Berry, R., Jeffery, E., Rodeheffer, M.S., 2014. Weighing in on adipocyte precursors. Cell Metabolism 19:8—20.

[31] Moldes, M., Lasnier, F., Feve, B., Pairault, J., Djian, P., 1997. Id3 prevents differentiation of preadipose cells. Molecular and Cellular Biology 17:1796—1804.

[32] O'Brien, C.A., Kreso, A., Ryan, P., Hermans, K.G., Gibson, L., Wang, Y., et al., 2012. ID1 and ID3 regulate the self-renewal capacity of human colon cancer-initiating cells through p21. Cancer Cell 21:777—792.

[33] Waga, S., Hannon, G.J., Beach, D., Stillman, B., 1994. The p21 inhibitor of cyclin-dependent kinases controls DNA replication by interaction with PCNA. Nature 369:574—578.

[34] Yu, R., Kim, C.S., Kwon, B.S., Kawada, T., 2006. Mesenteric adipose tissue-derived monocyte chemoattractant protein-1 plays a crucial role in adipose tissue macrophage migration and activation in obese mice. Obesity (Silver Spring) 14:1353—1362.

[35] Mitterberger, M.C., Lechner, S., Mattesich, M., Kaiser, A., Probst, D., Wenger, N., et al., 2012. DLK1(PREF1) is a negative regulator of adipogenesis in CD105(+)/CD90(+)/CD34(+)/CD31(−)/FABP4(−) adipose-derived stromal cells from subcutaneous abdominal fat pats of adult women. Stem Cell Research 9:35—48.

[36] Perez, L.M., Bernal, A., San Martin, N., Galvez, B.G., 2013. Obese-derived ASCs show impaired migration and angiogenesis properties. Archives in Physiology and Biochemistry 119:195—201.

[37] Weisberg, S.P., Hunter, D., Huber, R., Lemieux, J., Slaymaker, S., Vaddi, K., et al., 2006. CCR2 modulates inflammatory and metabolic effects of high-fat feeding. Journal of Clinical Investigation 116:115—124.

[38] Fain, J.N., 2006. Release of interleukins and other inflammatory cytokines by human adipose tissue is enhanced in obesity and primarily due to the nonfat cells. Vitamins & Hormones 74:443—477.

[39] Cushing, S.D., Berliner, J.A., Valente, A.J., Territo, M.C., Navab, M., Parhami, F., et al., 1990. Minimally modified low density lipoprotein induces monocyte chemotactic protein 1 in human endothelial cells and smooth muscle cells. Proceedings of the National Academy of Sciences of the United States of America 87:5134—5138.

[40] Schipper, H.S., Prakken, B., Kalkhoven, E., Boes, M., 2012. Adipose tissue-resident immune cells: key players in immunometabolism. Trends in Endocrinology & Metabolism 23:407—415.

[41] Fantin, A., Vieira, J.M., Gestri, G., Denti, L., Schwarz, Q., Prykhozhij, S., et al., 2010. Tissue macrophages act as cellular chaperones for vascular anastomosis downstream of VEGF-mediated endothelial tip cell induction. Blood 116:829—840.

[42] Pucci, F., Venneri, M.A., Biziato, D., Nonis, A., Moi, D., Sica, A., et al., 2009. A distinguishing gene signature shared by tumor-infiltrating Tie2-expressing monocytes, blood "resident" monocytes, and embryonic macrophages suggests common functions and developmental relationships. Blood 114:901—914.

[43] Nakao, S., Kuwano, T., Tsutsumi-Miyahara, C., Ueda, S., Kimura, Y.N., Hamano, S., et al., 2005. Infiltration of COX-2-expressing macrophages is a prerequisite for IL-1 beta-induced neovascularization and tumor growth. Journal of Clinical Investigation 115:2979—2991.

[44] Tang, W., Zeve, D., Suh, J.M., Bosnakovski, D., Kyba, M., Hammer, R.E., et al., 2008. White fat progenitor cells reside in the adipose vasculature. Science 322:583—586.

[45] Tran, K.V., Gealekman, O., Frontini, A., Zingaretti, M.C., Morroni, M., Giordano, A., et al., 2012. The vascular endothelium of the adipose tissue gives rise to both white and brown fat cells. Cell Metabolism 15:222—229.

[46] Han, J., Lee, J.E., Jin, J., Lim, J.S., Oh, N., Kim, K., et al., 2011. The spatiotemporal development of adipose tissue. Development 138:5027—5037.

[47] Valet, P., Tavernier, G., Castan-Laurell, I., Saulnier-Blache, J.S., Langin, D., 2002. Understanding adipose tissue development from transgenic animal models. Journal of Lipid Research 43:835—860.

[48] Jeffery, E., Church, C.D., Holtrup, B., Colman, L., Rodeheffer, M.S., 2015. Rapid depot-specific activation of adipocyte precursor cells at the onset of obesity. Nature Cell Biology 17:376—385.

[49] Fujiwara, K., Hasegawa, K., Ohkumo, T., Miyoshi, H., Tseng, Y.H., Yoshikawa, K., 2012. Necdin controls proliferation of white adipocyte progenitor cells. PLoS One 7:e30948.

Original article

[50] Naaz, A., Holsberger, D.R., Iwamoto, G.A., Nelson, A., Kiyokawa, H., Cooke, P.S., 2004. Loss of cyclin-dependent kinase inhibitors produces adipocyte hyperplasia and obesity. FASEB Journal 18:1925—1927.

[51] Kirk, E.A., Sagawa, Z.K., McDonald, T.O., O'Brien, K.D., Heinecke, J.W., 2008. Monocyte chemoattractant protein deficiency fails to restrain macrophage infiltration into adipose tissue [corrected]. Diabetes 57:1254—1261.

[52] Oh, D.Y., Morinaga, H., Talukdar, S., Bae, E.J., Olefsky, J.M., 2012. Increased macrophage migration into adipose tissue in obese mice. Diabetes 61:346—354.

[53] Chen, G.Y., Chen, X., King, S., Cavassani, K.A., Cheng, J., Zheng, X., et al., 2011. Amelioration of sepsis by inhibiting sialidase-mediated disruption of the CD24-SiglecG interaction. Nature Biotechnology 29:428—435.

[54] Zhou, Q., Rammohan, K., Lin, S., Robinson, N., Li, O., Liu, X., et al., 2003. CD24 is a genetic modifier for risk and progression of multiple sclerosis. Proceedings of the National Academy of Sciences of the United States of America 100:15041—15046.

[55] Fang, X., Zheng, P., Tang, J., Liu, Y., 2010. CD24: from A to Z. Cellular & Molecular Immunology 7:100—103.

[56] Suzuki, T., Kiyokawa, N., Taguchi, T., Sekino, T., Katagiri, Y.U., Fujimoto, J., 2001. CD24 induces apoptosis in human B cells via the glycolipid-enriched membrane domains/rafts-mediated signaling system. Journal of Immunology 166:5567—5577.

[57] Perez, L.M., Bernal, A., San Martin, N., Lorenzo, M., Fernandez-Veledo, S., Galvez, B.G., 2013. Metabolic rescue of obese adipose-derived stem cells by Lin28/Let7 pathway. Diabetes 62:2368—2379.

[58] Gesta, S., Bluher, M., Yamamoto, Y., Norris, A.W., Berndt, J., Kralisch, S., et al., 2006. Evidence for a role of developmental genes in the origin of obesity and body fat distribution. Proceedings of the National Academy of Sciences of the United States of America 103:6676—6681.

[59] Tchkonia, T., Lenburg, M., Thomou, T., Giorgadze, N., Frampton, G., Pirtskhalava, T., et al., 2007. Identification of depot-specific human fat cell progenitors through distinct expression profiles and developmental gene patterns. American Journal of Physiology-Endocrinology and Metabolism 292:E298—E307.

[60] Cancello, R., Tordjman, J., Poitou, C., Guilhem, G., Bouillot, J.L., Hugol, D., et al., 2006. Increased infiltration of macrophages in omental adipose tissue is associated with marked hepatic lesions in morbid human obesity. Diabetes 55: 1554—1561.

[61] Jiang, D., Liang, J., Noble, P.W., 2011. Hyaluronan as an immune regulator in human diseases. Physiology Reviews 91:221—264.

[62] Sun, J., Feng, A., Chen, S., Zhang, Y., Xie, Q., Yang, M., et al., 2013. Osteopontin splice variants expressed by breast tumors regulate monocyte activation via MCP-1 and TGF-beta1. Cellular & Molecular Immunology 10: 176—182.

[63] Kahles, F., Findeisen, H.M., Bruemmer, D., 2014. Osteopontin: a novel regulator at the cross roads of inflammation, obesity and diabetes. Molecular Metabolism 3:384—393.

[64] Nomiyama, T., Perez-Tilve, D., Ogawa, D., Gizard, F., Zhao, Y., Heywood, E.B., et al., 2007. Osteopontin mediates obesity-induced adipose tissue macrophage infiltration and insulin resistance in mice. Journal of Clinical Investigation 117:2877—2888.

[65] Han, C.Y., Subramanian, S., Chan, C.K., Omer, M., Chiba, T., Wight, T.N., et al., 2007. Adipocyte-derived serum amyloid A3 and hyaluronan play a role in monocyte recruitment and adhesion. Diabetes 56:2260—2273.

[66] Kodama, K., Horikoshi, M., Toda, K., Yamada, S., Hara, K., Irie, J., et al., 2012. Expression-based genome-wide association study links the receptor CD44 in adipose tissue with type 2 diabetes. Proceedings of the National Academy of Sciences of the United States of America 109:7049—7054.

[67] Grundy, S.M., 2002. Obesity, metabolic syndrome, and coronary atherosclerosis. Circulation 105:2696—2698.

[68] Vucenik, I., Stains, J.P., 2012. Obesity and cancer risk: evidence, mechanisms, and recommendations. Annals of the New York Academy of Sciences 1271:37—43.

[69] Procaccini, C., Carbone, F., Galgani, M., La Rocca, C., De Rosa, V., Cassano, S., et al., 2011. Obesity and susceptibility to autoimmune diseases. Expert Review of Clinical Immunology 7:287—294.

[70] Wernstedt Asterholm, I., Tao, C., Morley, T.S., Wang, Q.A., Delgado-Lopez, F., Wang, Z.V., et al., 2014. Adipocyte inflammation is essential for healthy adipose tissue expansion and remodeling. Cell Metabolism 20:103—118.